Renewable and Sustainable Energy Reviews 21 (2013) 59–83

Contents lists available at SciVerse ScienceDirect

Renewable and Sustainable Energy Reviews

journal homepage: www.elsevier.com/locate/rser

Energetic and exergetic aspects of solar air heating (solar collector) systems

Hakan F. Oztop [a,*], Fatih Bayrak [b], Arif Hepbasli [c]

[a] Department of Mechanical Engineering, Technology Faculty, Fırat University, TR-23119 Elazig, Turkey
[b] Department of Mechanical Education, Technical Education Faculty, Fırat University, TR-23119 Elazig, Turkey
[c] Department of Energy Systems Engineering, Faculty of Engineering, Yaşar University, 35100 Bornova, Izmir, Turkey

A R T I C L E I N F O

Article history:
Received 18 April 2011
Received in revised form
22 October 2012
Accepted 21 December 2012
Available online 24 January 2013

Keywords:
Solar energy
Solar air heater
Exergy
Heat transfer enhancement
Renewable energy

A B S T R A C T

Solar air heating (solar collector) is a renewable heating technology and provides heat using solar energy. With fuel costs and other factors, solar air heaters (SAHs) are getting more attention. The energetic and exergetic performance of SAHs is influenced by a number of factors. The present study reviews the previously conducted studies and applications in terms of design, performance assessment, heat transfer enhancement techniques, experimental and numerical works, thermal heat storage, effectiveness compassion and recent advances. It may be concluded that energy analysis method has been used in a number of studies while exergy analysis method has been applied to the relatively low numbers of systems. Energy efficiencies of solar air collectors reviewed varied from 47% and 89%. It is expected that this comprehensive study will be very beneficial to everyone involved or interested in the energetic and exergetic design, simulation, analysis, test and performance assessment of SAHs.

Contents

1. Introduction

The simplest and most efficient way to utilize solar energy is to convert it into thermal energy for heating applications using solar collectors. Solar air heaters (SAHs) are cheap and have been widely used for years because of their inherent simplicity. They are a kind of heat exchangers that transform solar energy into heat. Most advantages of these systems are freezing or boiling of the fluid does not occur. Disadvantages are, however, the low density, the low thermal capacity and the small heat conductivity of air. The main applications of SAHs are space heating, seasoning of timber, curing of industrial products, and these can also be effectively used for curing/drying of concrete/clay building components. The SAH occupies an important

* Corresponding author. Tel.: +90 424 237 0000x4222; fax: +90 424 236 7024.
E-mail addresses: hfoztop1@gmail.com (H.F. Oztop),
fatih.byrk@gmail.com (F. Bayrak),
arif.hepbasli@yasar.edu.tr (A. Hepbasli).

1364-0321/$ - see front matter
http://dx.doi.org/10.1016/j.rser.2012.12.019

Nomenclature

A_c	surface area of the collector (m^2)
C_p	specific heat of air at constant pressure (kJ/kg K)
$\dot{E}$	energy rate (kW)
$\dot{E}_X$	exergy rate (kW)
h	enthalpy (kJ/kg)
I	solar radiation (W/m^2)
$I\dot{P}$	rate of improvement potential (kW)
$\dot{m}$	mass flow rate (kg/s)
M	mass (kg)
P	fluid pressure (Pa)
R	universal gas constant (J/kg K)
R	regression coefficients (dimensionless)
$\dot{Q}_c$	heat rate (kW)
s	entropy (kJ/kg K)
$\dot{S}$	entropy generation rate (kW/kg K)
T	temperature (°C)
U	heat loss coefficient (W/m^2 °C)
$\dot{W}$	work rate or power (kW)
W	uncertainty in the measurement (%)
I_T	incident solar energy per absorber area unit ($kW\,m^{-2}$)
Nu	Nusselt number$=hD_h/k$
f	fanning friction factor
p	reflectivity of the absorber
τ	transmissivity of the absorber
$\tau\alpha$	effective product transmittance–absorptance

Greek letters

α	absorptivity (dimensionless)
η_{I}	thermal efficiency (dimensionless)
η_{II}	exergetic efficiency (dimensionless)
η_o	optical yield (dimensionless)
ψ	specific exergy (kJ/kg)

Subscripts

a	air
ave	average
C	collector
D	dimensionless
c	convection
dest	destroyed
f	fluid
in	inlet
m	mean
out	outlet
p	plate
r	radiation
s	sun, sun temperature, smooth duct
G	glass

place among solar heating system because of minimal use of materials and cost [1,2]. The applications of solar energy to heat the fluids can include drying vegetables, fruits, meats, eggs incubation, and other industrial purposes [3]. SAHs are also integrated with photovoltaic (PV) systems to produce both thermal energy and electricity, which are called as PV/T collectors [4]. Some important advantages of solar thermal systems are as follows: they work on noiseless environment, do not produce any unwanted waste such as radioactive materials and are one of clean technologies. They do not produce any toxic waste or radioactive material and are highly credible systems with life span expectation between 20 and 30 years. They are also low maintenance systems. Non-uniform cooling – need innovative absorber design, payback – less efficiency, longer payback period, production and installation cost-expensive and high cost, not suitable for integration with present roof system and need larger space for separate systems (hot water and electricity production) are some disadvantages of solar systems.

SAHs are also used to heat spaces, especially during autumn and spring seasons. As stated above that their efficiencies are still lower compared to other systems. Thus, there are many studies on heat transfer enhancement technique of SAHs such as surface treatment, attaching of different shaped baffles or fins, changing of flow directions etc. in the literature. In the recent years, many studies have focused on enhancement of heat transfer in SAHs and constructing of high efficiency collectors. Various studies have been undertaken using numerical and experimental methods, while results obtained have been used to calculate energy and exergy efficiency of SAHs.

2. Historical development of solar air collectors

Solar energy has been used since time immemorial to dry agricultural products, to provide space heat in cold seasons or to create ventilation in homes, applications, which are still used in many developing countries. More than two thousand years ago, Heron of Alexandria constructed a simple water pump driven by solar energy, and in 214 B.C., Archimedes of Syracuse used concentrating solar mirrors to set fire to Roman ships [5]. By 1870, John Ericsson, one of the most influential and controversial U.S. engineers of the nineteenth century, had developed what he claimed to be the first solar-powered steam engine. There are records of solar collectors in the United States dating back to before 1900, comprising a black-painted tank mounted on a roof. In 1896 Clarence Kemp of Baltimore, USA enclosed a tank in a wooden box, thus creating the first ‘batch water heater’ as they are known today. Although flat-plate collectors for solar water heating were used in Florida and Southern California in the 1920s there was a surge of interest in solar heating in North America after 1960, but specially after the 1973 oil crisis.

By the mid-1980s, contemporary solar engineers determined that for sunny areas, tracking parabolic troughs were the best compromise because they exhibited superior cost/power ratios in most locations. In 1978, studies on research and development of the line focus parabolic trough concentrator were begun [6]. The first Commercial solar power plants have been in operation in California since the mid-1980s, providing the 354 MW of the world’s lowest-cost solar power [7]. Interest in commercializing concentrating solar technologies has been rejuvenated, after a first phase of success in the late-1980s [8].

3. Classification of solar air collectors

SAHs are classified according to collector cover, absorber materials, shape of absorbing surface, absorber flow pattern, flow shapes, hybrid collectors and their applications. All challenges have focused on heat transfer enhancement inside the SAHs. A classification of SAHs is given in Fig. 1 where each group is divided into sub-classifications.

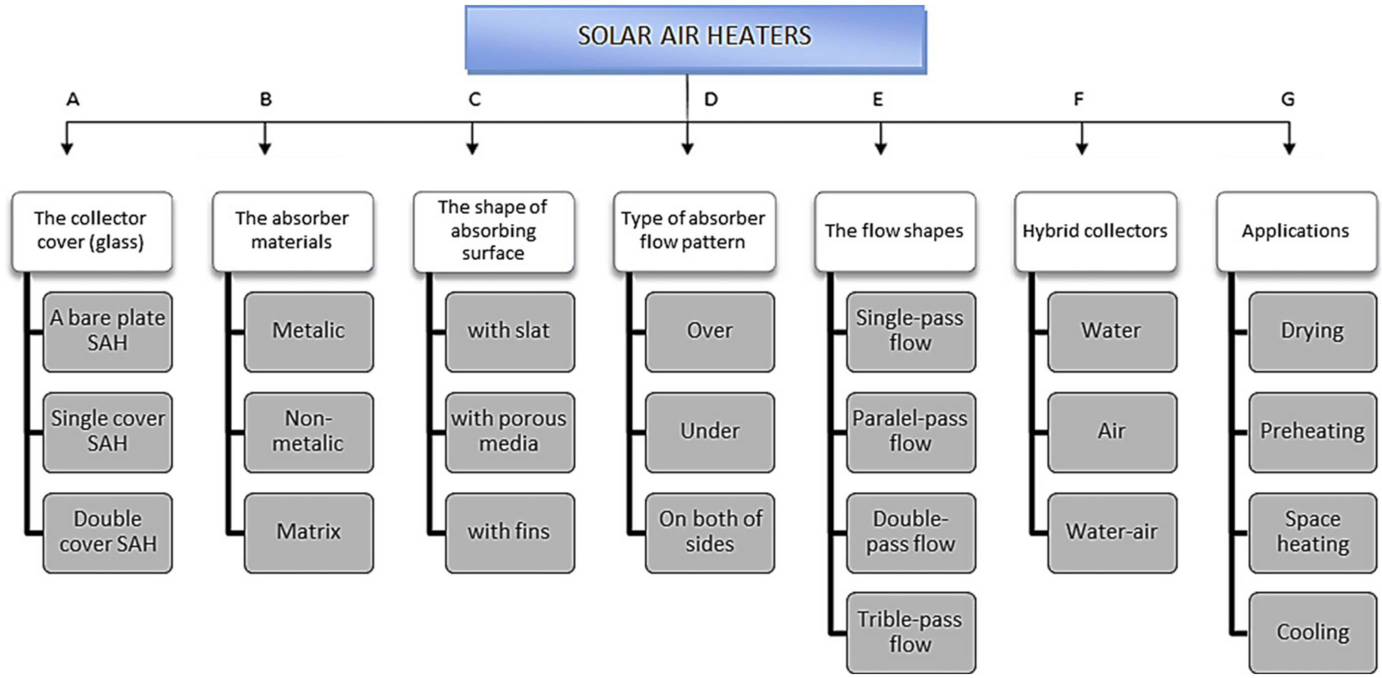

Fig. 1. Classification of collectors.

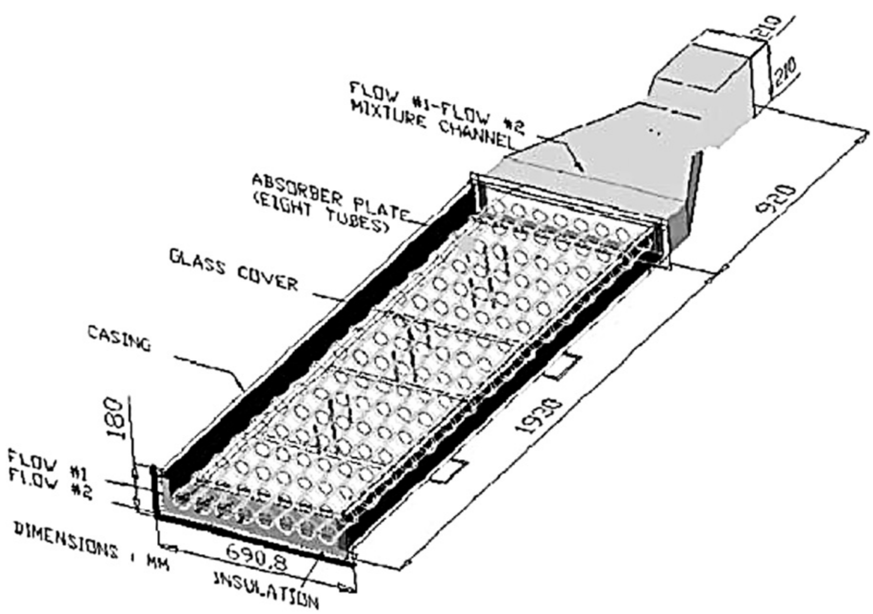

Fig. 2. Schematic diagram of the air solar collector [10].

4. Brief theory on solar air collector performance

Calculation of the solar collector efficiency according to the first law is defined as the ratio of the energy gain to the solar radiation incident on the collector plane as follows [9]:

$$\eta = \frac{\dot{Q}_c}{\dot{Q}_s} \tag{1}$$

where $\dot{Q}_c$ is the rate of heat transfer to a working fluid in the solar collector, and $\dot{Q}_s$ the solar energy absorbed by the solar collector surface, as given below:

$$\dot{Q}_s = I_T(\tau\alpha)A_c \tag{2}$$

where I_T is the rate of incidence of radiation per unit area of the tilted collector surface, A_c the collector area, and $\tau\alpha$ the effective product transmittance–absorptance. Value of $\tau\alpha$ represents the fraction of the solar radiation absorbed by the collectors and depends mainly on the transmittance of the transparent covers and on the absorbance of the absorbent. The effective product transmittance–absorptance can be evaluated using

$$(\tau\alpha) = \frac{\tau\alpha}{1-(1-\alpha)}\rho_G \tag{3}$$

Eq. (1) gives the results of a first law analysis of flat plate solar collectors because all energy fluxes are treated equally, regardless of their potential usefulness. The absorption heat-transfer rate by

the solar collectors, $\dot{Q}_c$, can be estimated from

$$\dot{Q}_c = \dot{m}_a C_{pa}(T_{a,out} - T_{a,in}) \tag{4}$$

5. Surface enhancement techniques

Efficiency of SAHs is still low to produce enough thermal energy. Thus, some active and passive heat transfer enhancement techniques are applied to SAHs. Alvarez et al. [10], studied on the thermal performance of an air solar collector with an absorber plate made of recyclable aluminum cans. The absorber surface, which is the most important part of the solar air collector, consisted of eight circular cross sections air flow channels made of 128 Recyclable Aluminum Cans (RACs) painted in black. Their results showed that the efficiency increase of air solar collector using recyclable aluminum cans was technically and economically feasible if an adequate design was applied (Fig. 2) while a comparison of thermal efficiencies given by various authors is illustrated in Fig. 3 as given Ref. [10]. From this figure, the RAC air solar collector shows an intercept increase of 26.2%.

A novel solar air collector of pin-fin integrated absorber was designed by Peng et al. [11] to increase the thermal efficiency. Through analyzing the experimental results, the heat transfer coefficients on pin-fin arrays collectors and flat-plate collector were obtained under an air volume flow rate of 19 m^3/h and a

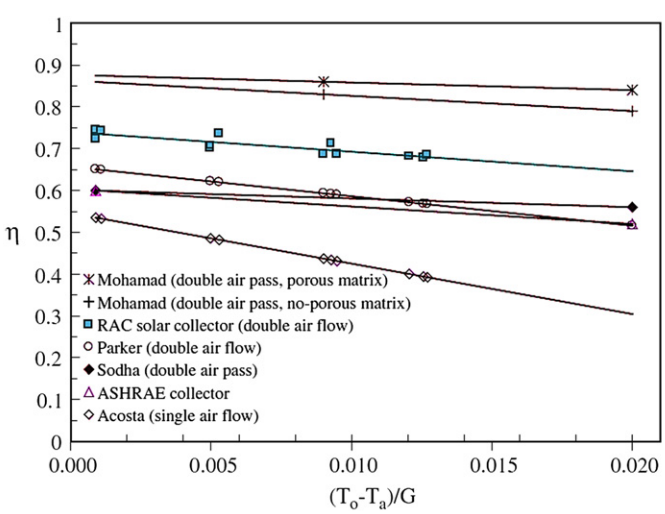

Fig. 3. Comparison between the thermal efficiency of the RAC air solar collector and the reported ones [10].

heat transfer coefficient of PZ3-11.25 pin-fins collector can reach three times than that of the flat-plate collector, as illustrated in Fig. 4. From Ref. [11]

An equation for this type of collector is given as

$$N_u = C\, Re^n\, Pr^m \tag{5}$$

Fig. 4 also makes a comparison between pin-fin and flat-plate collectors [11]. Garg et al. [12] investigated the effect of the rectangular ducts through which air flows in SAHs on the air heater performance for laminar, transitional and turbulent flows. Caner et al. [13] compared the two types of solar air collectors (Zigzagged absorber surface and Flat absorber surface) and from their performance point of view. They used artificial neural network model to estimate the thermal performances of solar air collectors. As seen from Fig. 5, they constructed two different solar air collectors using same properties of materials. They called these models as absorbing surface model (Fig. 5(a)) and straight surface model (Fig. 5(b)) [13].

Esen [14] presented a paper on energy and exergy analysis for a novel flat plate solar air collector with or without obstacles. The main aim of his study was to enhance the performance of solar air collector by enhancing heat transfer surface. They found that the largest irreversibility occurred at the flat plate (without obstacles) collector in which collector efficiency was smallest. Some pictures of these collectors are shown in Fig. 6(a)–(d) at Ref. [14].

The chevron pattern of fold structure produced using a recently developed continuous folding technique was considered for the first time in the application of solar air collectors by El-Sawi et al. [15]. The chevron pattern was found to have higher performance, reaching up to 20% improvement in thermal efficiency and an increase of 10 °C in outlet temperature at some ranges of mass flow rates. They designed two collector frames and manufactured to test both absorber plate configurations simultaneously to assure identical climate conditions at the time of the test as given in Fig. 7 from [15]. The effect of the mass flow rate on the outlet temperature as well as the efficiency of the solar collector is presented in Fig. 8 from [15]. As seen in the figure, the outlet temperature tended to decrease as the mass flow rate increased, where it was evident that the efficiency of the two collectors increased at slowing rate.

Ucar and Inallı [16] made an experimental work to enhance heat transfer by inserting short plates inside to the SAH. They indicated that one of the main disadvantages of solar air collectors in practical applications was their relatively low efficiency. In their experimental investigation, the shape and arrangement of absorber surfaces of the collectors were reorganized to provide better heat transfer surfaces suitable for the passive heat transfer

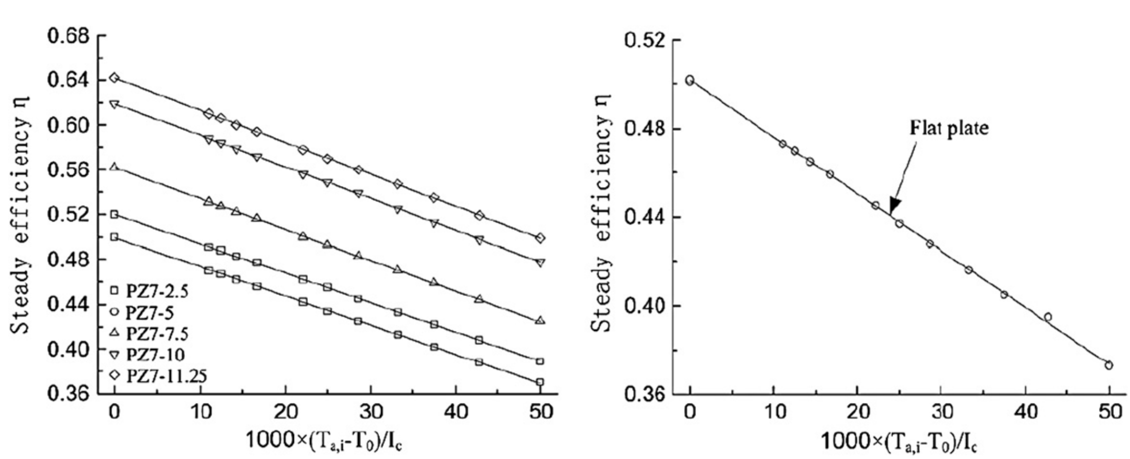

Fig. 4. Calculated efficiencies of pin-fin and flat-plate collectors by Peng et al. [11].

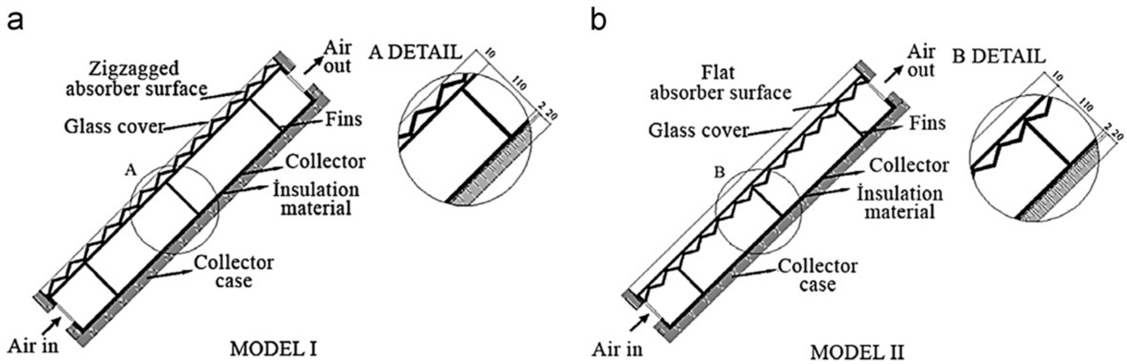

Fig. 5. (a) Zigzagged absorbed surface type and (b) flat absorber surface [13].

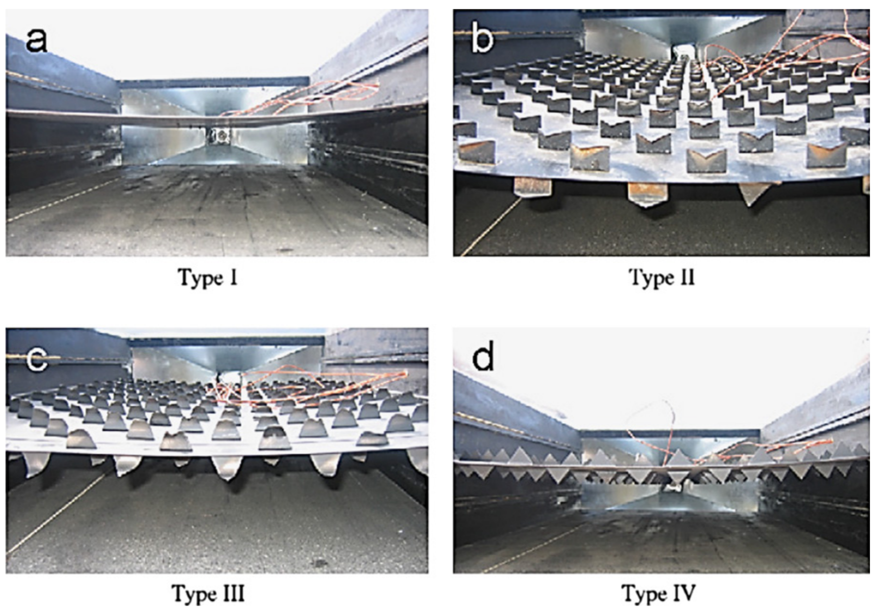

Fig. 6. Four types of plates in solar air heater (a) type I, (b) type II, (c) type III, and (d) type IV [14].

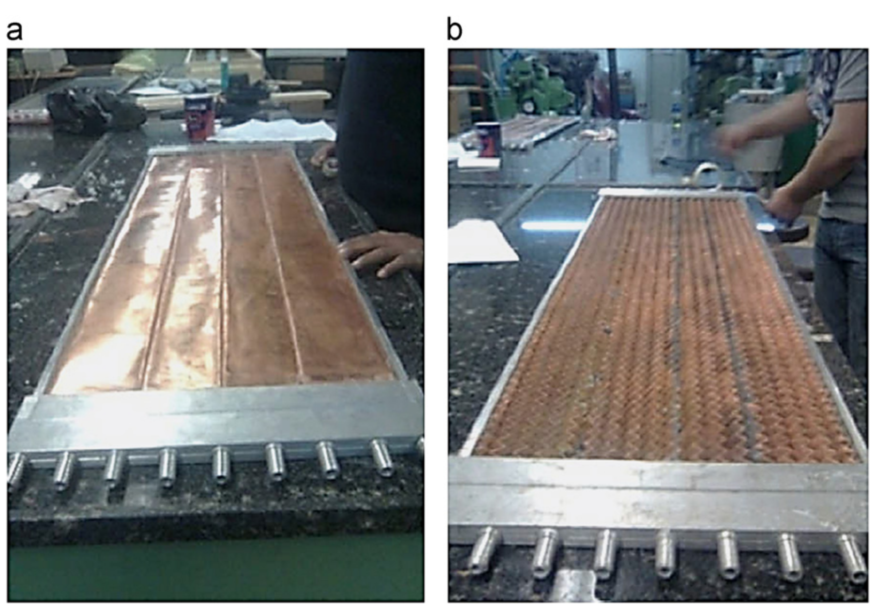

Fig. 7. Schematic of two types of collectors: (a) flat plate and (b) chevron plate [15].

augmentation techniques. It was found that the largest irreversibility occurred at the conventional solar collector in which collector efficiency was smallest. Their models are shown in Fig. 9 from [16].

Karsli [9] studied the performance analysis of four types (Fig. 10) of air heating flat plate solar collectors: a finned collector with an angle of 75°, a finned collector with an angle of 70°, a collector with tubes, and a base collector. In his study, the first and second laws of efficiencies were determined for the collectors and comparisons were made among them. They made a comparison of the collectors on the basis of first law and second law efficiencies in Fig. 11(a) and (b) from Ref. [9]. It was observed that the first law of efficiency changed between 26% and 80% for collector-I, between 26% and 42% for collector-II, between 70% and 60% for collector-III, and between 26% and 64% for collector-IV. The highest collector efficiency and air temperature rise were achieved by the finned collector with angle of 75°, whereas the lowest values were obtained for the base collector.

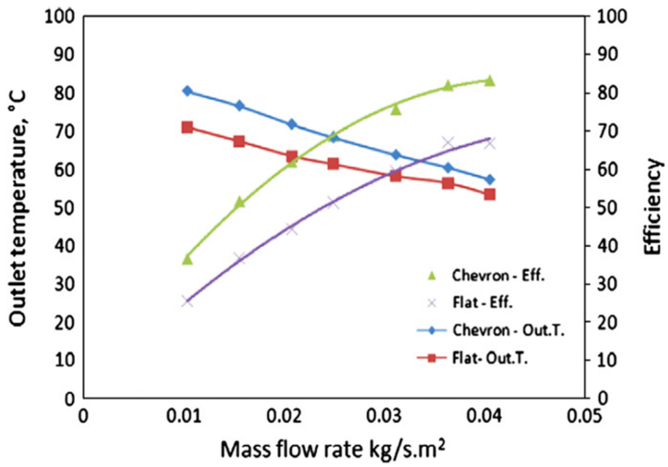

Fig. 8. Outlet temperature and efficiency vs. mass flow rate at T_i=42 °C, T_a=38 °C from Ref. [15].

Karim and Hawlader [17] studied on performance of v-groove solar air collector for drying applications, as shown in Fig. 12(a) and (b). Experimental results indicated better thermal efficiencies for a v-corrugated collector compared to a flat plate collector. Effects of operating variables on the thermal performance were investigated. The results showed that the temperature of the fluid at the exit of the collector decreased with flow rate resulting in an increase of efficiency due to the decreased thermal losses to the environment.

Experimental and analytical results indicated a good thermal performance of a v-groove collector. Satisfactory qualitative and quantitative agreement between experimental and analytical results was achieved.

Moummi et al. [18] carried out a work to improve the thermal performances of the solar air collector for some applications. Their configuration is presented in Fig. 13 as given in Ref. [18]. Initially, to improve the efficiency factor of these solar collectors, they created an increasingly turbulent flow between the absorber

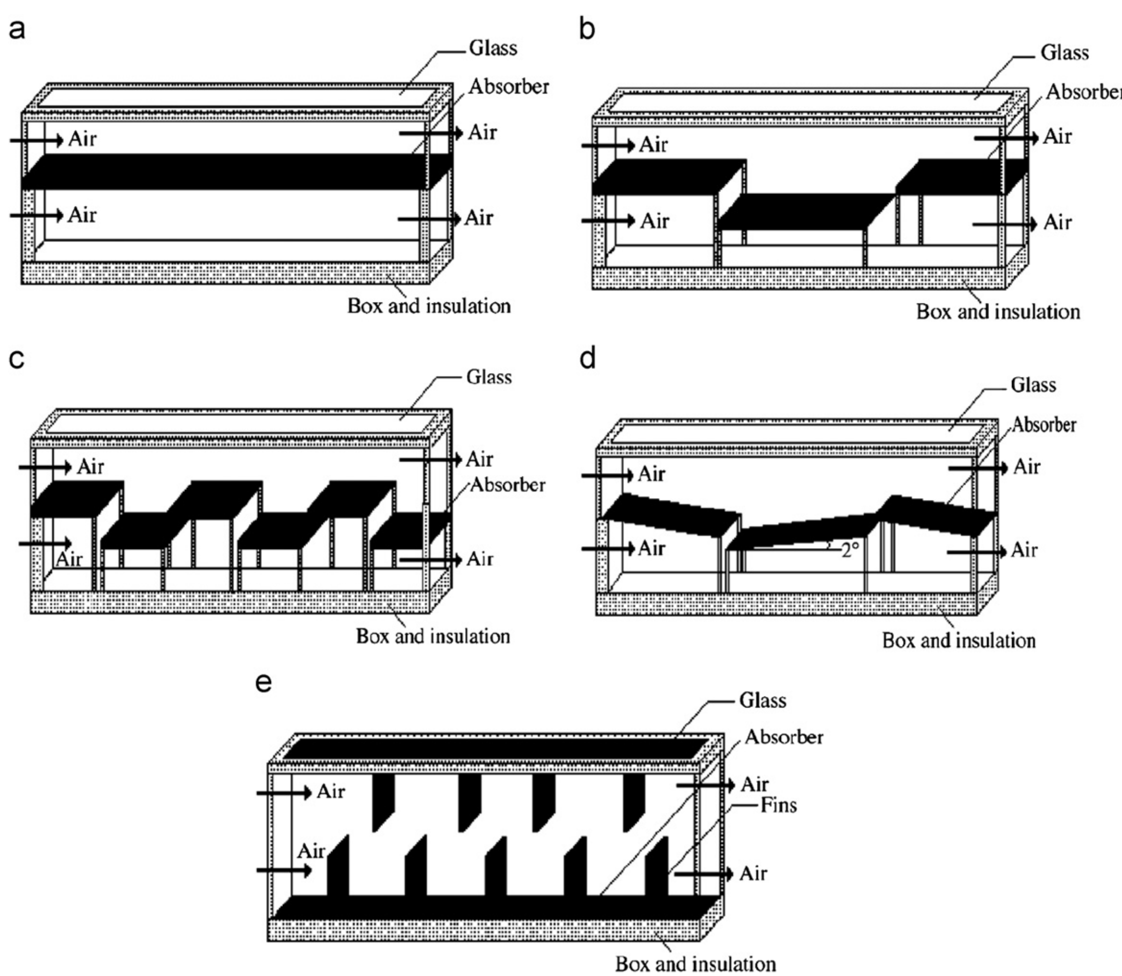

Fig. 9. Cross-sectional views of the tested solar air collectors (a) Type A, (b) Type B, (c) Type C, (d) Type D, and (e) Type E [16].

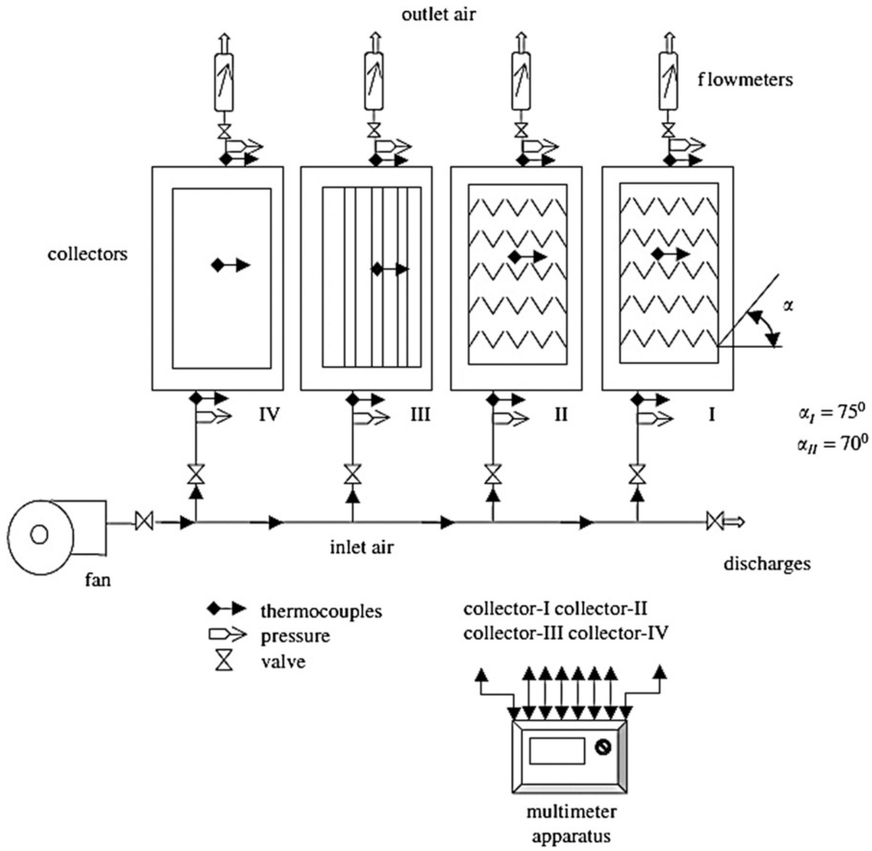

Fig. 10. Experimental setup [9].

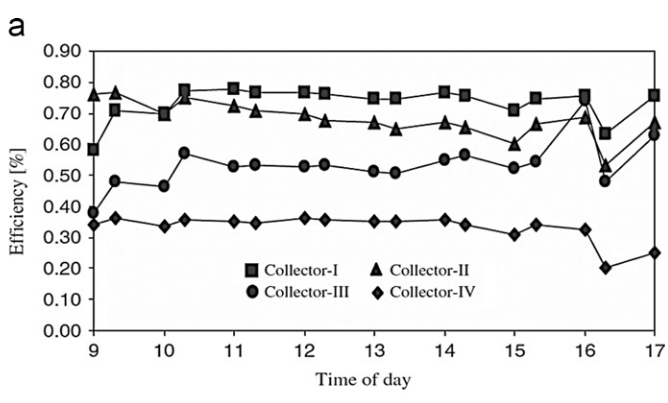

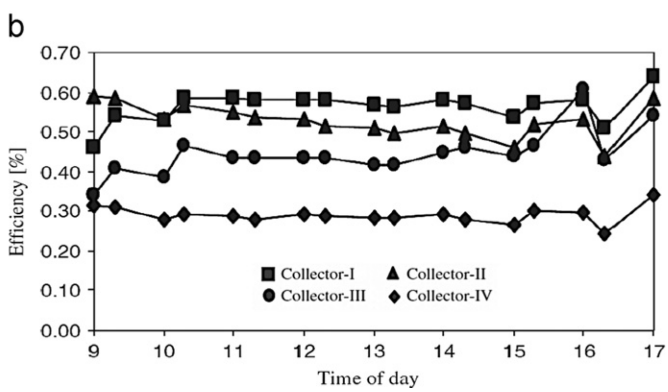

Fig. 11. Comparison of collectors on the basis of (a) first and (b) second law efficiencies [9].

and the back wooden plate. For that, they used obstacles of various forms. In this study, they utilized rectangular plate fins inserted perpendicular to the flow. The results were compared with those obtained with a solar air collector without fins, using two types of absorbers selective (in copper sun) or not selective (black-painted aluminum). In Fig. 14, volumetric flow rate was fixed at 35 m^3/h m^2, the enhancement of the efficiency was 30% for a collector provided with a selective absorber plate and 29% for a collector with a nonselective absorber plate [18].

Lalji et al. [19] made experimental work for generation of heat transfer and friction data for flow in a packed bed solar air heater at different mass flow rates of air for various porosities and shapes of matrices. On the basis of this investigation on heat transfer characteristics in packed bed solar air duct, it is concluded that the packed bed solar air heater having lower porosity performs better than higher porosity due to greater turbulence.

Objective of this paper is to review various studies, in which different artificial roughness elements are used to enhance the heat transfer coefficient with little penalty of friction factor [20]. On the basis of correlations developed by various investigators for heat transfer coefficient and friction factor, an attempt has been made to compare the thermohydraulic performance of roughened solar air heater ducts.

Sethi et al. [21] investigated experimental correlations for solar air heater duct with dimpled shape roughness elements on absorber plate. This study has been carried out for a range of system and operating parameters in order to analyse the effect of artificial roughness on heat transfer and friction characteristics in solar air heater duct which is having dimple shaped elements arranged in angular fashion (arc) as roughness elements on

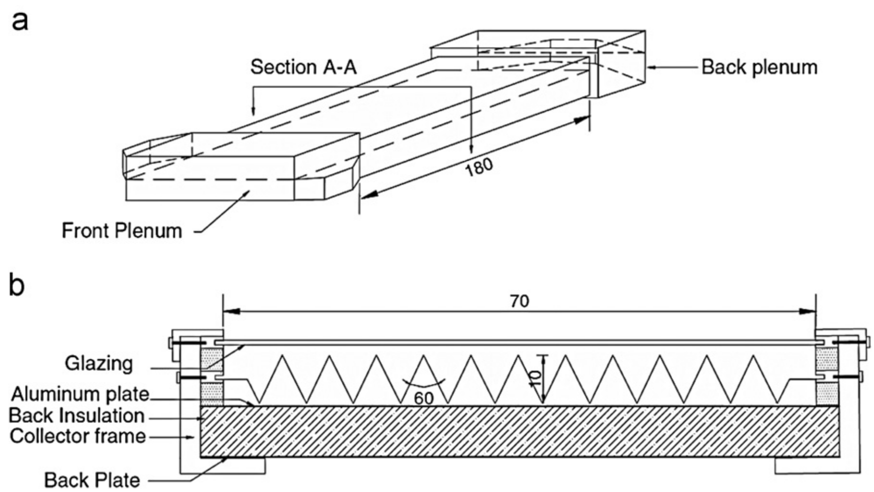

Fig. 12. Detail configuration of the test collector: (a) isometric view of the collector and (b) cross sectional view [17].

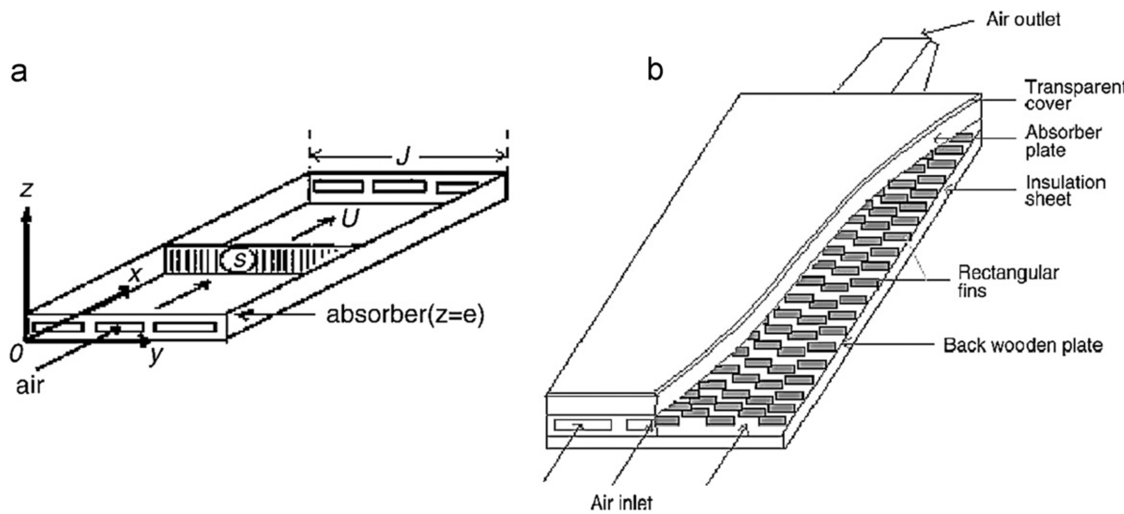

Fig. 13. (a) Detail in air channel duct and (b) collector with finned system on the back wooden plate [18].

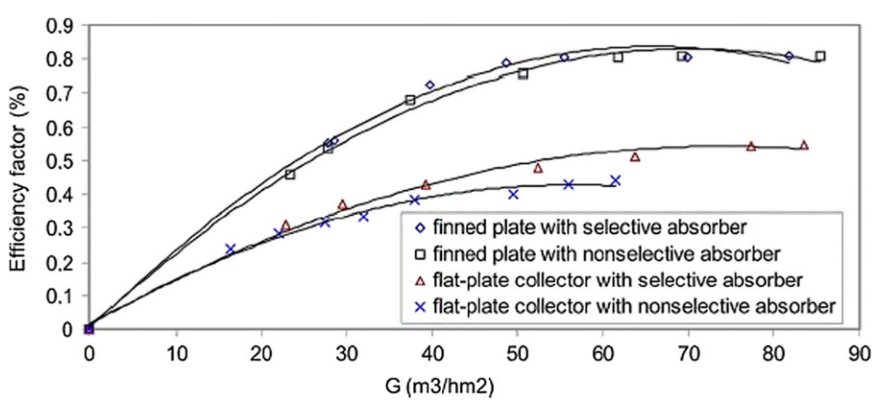

Fig. 14. Collector efficiency factor vs. the air volume flow rate for different configurations of collectors [18].

absorber plate. The experimental data have been used to develop Nusselt number and friction factor correlations as a function of roughness parameters and operating parameters.

Karim and Hawlader [22] made an experimental study of three types of solar air collectors, namely flat plate, finned and v-corrugated, towards achieving an efficient design of air collector suitable for a solar dryer as given in Fig. 15. The v-corrugated collector was found to be the most efficient collector and the flat plate collector the least efficient. Double pass operation of the collector resulted in further improvement of the efficiency compared to the single pass of operation. The improvement in efficiency for the double pass mode was most significant in the flat plate collector and least in the v-groove collector. The optimum operating conditions with respect to efficiency and the outlet temperature were determined for all three collectors given in Table 1 as given in Ref. [17]. The results indicated that for

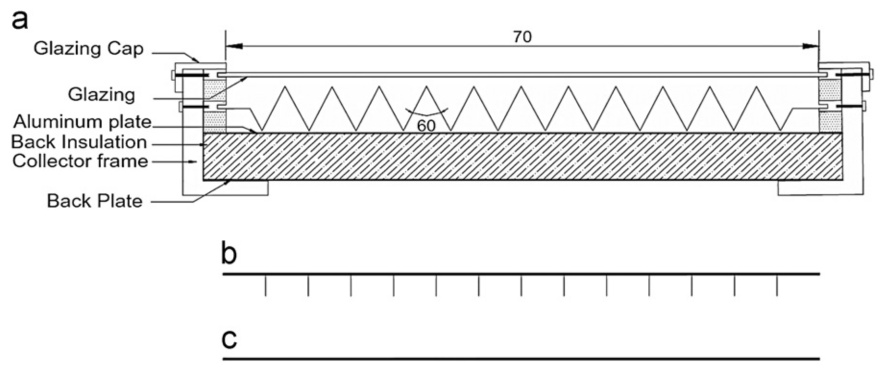

Fig. 15. Collector frame and three type of absorbers: (a) cross sectional view, (b) finned absorber, and (c) flat plate absorber [22].

Table 1
Optimum conditions of three collectors studied by Karim and Hawlader [17].

Collector type	Flow rate (kg/m^2 s)	Outlet temperature (°C)	Efficiency (%)
V-Groove	0.031	53	68.5
Finned	0.029	50	65.0
Flat plate	0.030	48	62.0

drying purposes, the designed air flow rate would be in the range of about 0.025–0.035 kg/m^2 s. This range of flow rate gave an outlet temperature suitable for most agricultural drying applications, and the corresponding efficiency was considered reasonable. Studies on heat transfer enhancement techniques can be found in Mittal and Varshney [23], who investigated the performance of SAHs theoretically while Hans et al. [24] analyzed the solar air collectors, which included v-shaped bars for 8 different types. They also developed a correlation between heat transfer and friction factor. Other studies related with heat transfer enhancement techniques in solar air collectors can be found in Refs. [25–80].

As indicated above that drying process is the most application area for solar air collectors. For some products, solar air collectors may be a single heat source or may assist in the drying process, as reported in Refs. [22,81–87].

6. Double pass solar collectors

Double pass counter flow solar air collector with porous material in the second air passage is one of the important and attractive design improvements that have been proposed to improve the thermal performance [88]. In this context, effects of various parameters on the thermal performance and pressure drop characteristics were discussed by Ramani et al. [88]. Their model is plotted in Fig. 16 [88]. They made both experimental and theoretical analysis. Comparison of the results indicated that the thermal efficiency of double pass solar air collector with porous absorbing material was 20–25% and 30–35% higher than that of double pass solar air collector without porous absorbing material and single pass collector respectively.

It was reported that the thermal efficiency of double pass solar air collector with porous material was higher than that of double pass solar air collector without porous material and conventional single pass collector. As a similar study, evaluation of thermal efficiency of double-pass solar air collector with porous–nonporous media was made by Sopian et al. [89]. The addition of the porous media in the second channel of the double-pass solar air collector increased the performance of the collector. This type of collector had a higher thermal performance compared to the conventional single-pass solar collector.

Ho et al. [90] studied the collector efficiency of upward-type double-pass flat plate SAHs with fins attached and external recycle was investigated theoretically, as shown in Figs. 17 and 18 [90]. The double-pass device was constructed by inserting the absorbing plate into the air conduit to divide it into two channels. The double-pass device introduced here was designed for creating a solar collector with heat transfer area double as well as the extended area of fins between the absorbing plate and heated air. The double-pass type SAHs was proposed in their study. They had the extended heat transfer area and the strengthened convective heat transfer coefficient, leading to improved thermal performance on the new device. It was shown that the desirable effect of increasing the fluid velocity using the recycling operation to overcome the undesirable driving force decreased (temperature difference) for heat transfer due to remixing at the inlet. Yeh and Ho [91] made another theoretical work on downward-type SAHs with internal recycle. They indicated that the performance in a SAH operated with internal recycle overcame that in the same size device operated with external recycle [92]. Effect of collector aspect ratio on the collector efficiency of upward type baffled SAHs was investigated by Yeh et al. [93]. In this case, although the collector efficiency of baffled SAHs was larger than that of flat plate heaters without fins and baffles, the improvement of collector efficiency by increasing the collector aspect ratio was reverse.

The double pass-finned plate SAH was investigated theoretically and experimentally by El-Sebaii et al. [94]. Comparisons between the measured outlet temperatures of flowing air, temperature of the absorber plate and output power of the double pass-finned and v-corrugated plate SAHs were presented. The effect of mass flow rates of air on pressure drop, thermal and thermohydraulic efficiencies of the double pass finned and v-corrugated plate SAHs were also investigated. The results showed that the double pass v-corrugated plate SAH was 9.3–11.9% more efficient compared to the double pass-finned plate SAH. It was also indicated that the peak values of the thermohydraulic efficiencies of the double pass-finned and v-corrugated plate SAHs were obtained when the mass flow rates of the flowing air equal 0.0125 and 0.0225 kg/s, respectively. As seen in Fig. 19 [91], the thermal efficiencies of DPFIPSAH and DPVCPSAH were 58% and 65.3%, respectively.

The thermal performance of a double-glass double-pass SAH with a packed bed (DPSAHPB) above the heater absorber plate was investigated experimentally and theoretically by Ramadan et al. [95]. Limestone and gravel were used as packed bed materials. It was inferred that for increasing the outlet temperature T_{flo} of the flowing air after sunset, it was advisable to use the packed bed materials with higher masses and therefore with low porosities. The thermohydraulic efficiency η_{TH} was found to increase with increasing $\dot{m}_f$ until a typical value of 0.05 kg/s

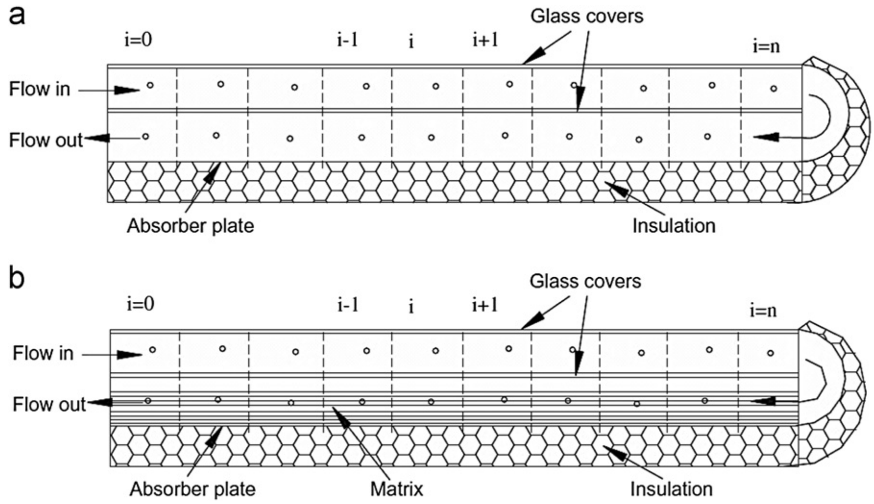

Fig. 16. Double pass arrangement: (a) without porous material and (b) with porous material [88].

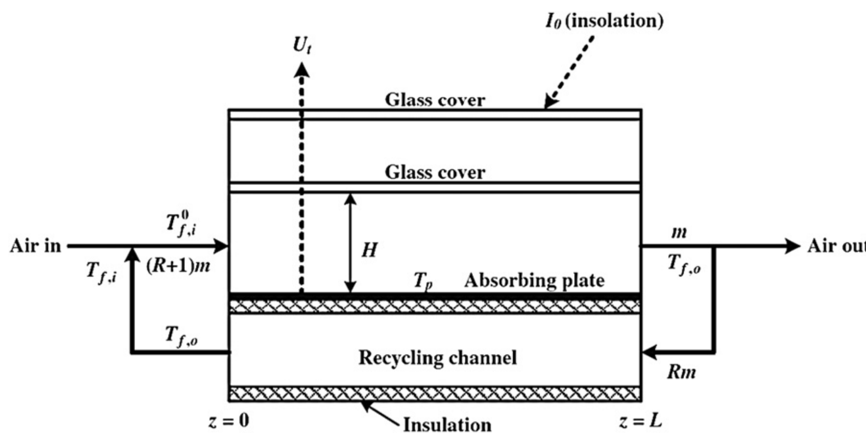

Fig. 17. Schematic diagram of a solar air heater [90].

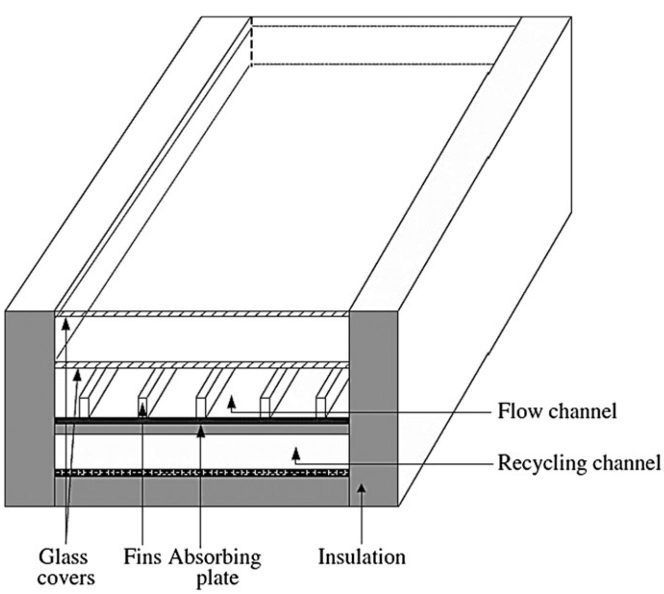

Fig. 18. Solar air heater with internal fins attached [90].

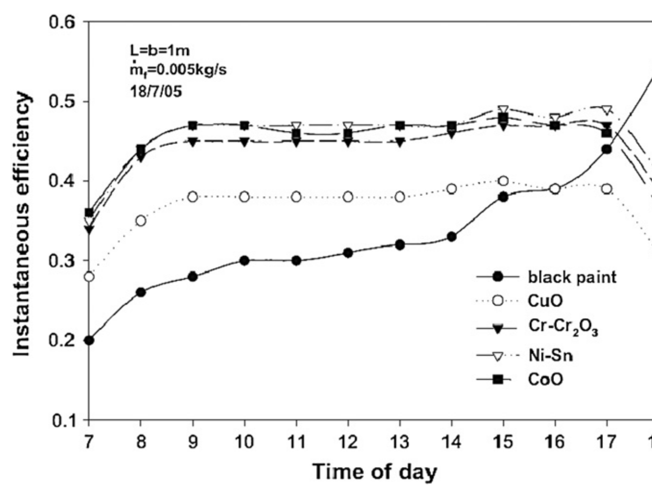

Fig. 19. Effect of mass flow rates of air $\dot{m}$ on the thermal efficiency of the double pass-finned (DPFIPSAH) and v-corrugated (DPVCPSAH) plate solar air heaters on a typical day of July 2009 [94].

beyond which the increase in η_{TH} becomes insignificant. It was recommended to operate the system with packed bed with values of $\dot{m}_f$ equal 0.05 kg/s or lower to have a lower pressure drop across the system. To validate the proposed mathematical model, based on comparisons between experimental and theoretical results, a good agreement was achieved. Fig. 20 shows variations of the thermohydraulic efficiency versus flow rate for the system

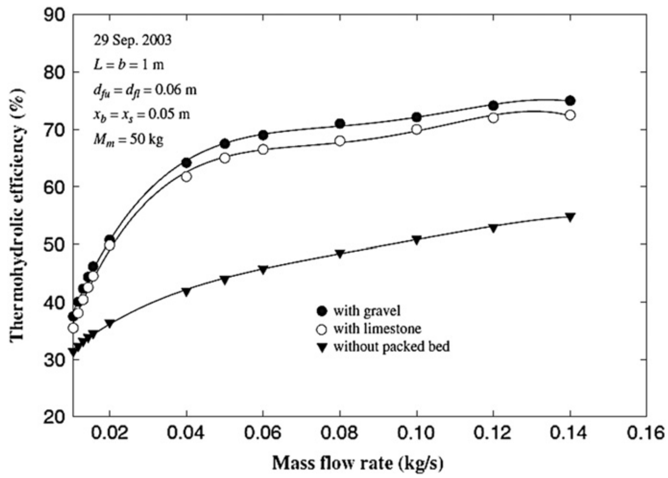

Fig. 20. Effect of mass flow rate of air $\dot{m}_f$ on the thermohydraulic efficiency η_{TH} without and with 50 kg limestone and gravel [95].

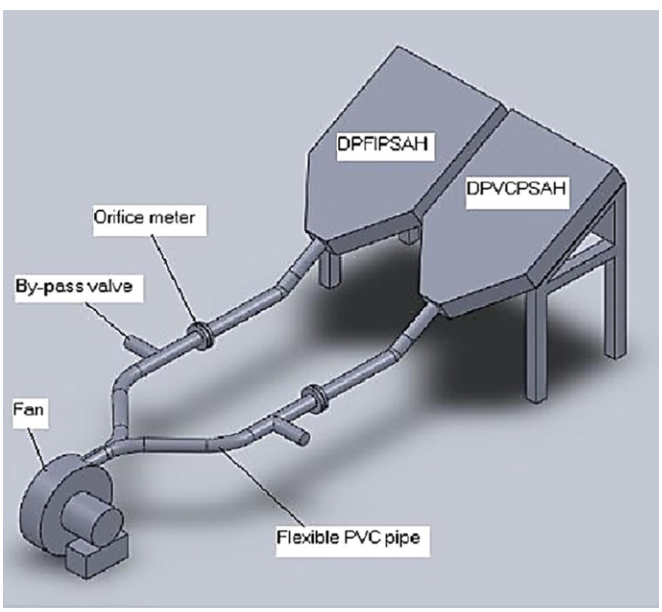

Fig. 21. Schematic diagram of the air solar collector [96].

without and with gravel and limestone as packed bed [95]. As seen in the figure, the efficiency was strongly related with flow rate.

El-Sebaii et al. [96] studied the double pass flat and v-corrugated plate SAHs theoretically and experimentally. Experimental set-up is presented in Fig. 21 from Ref. [96]. Comparisons between the measured outlet temperatures of flowing air, output power and overall heat losses of the flat and v-corrugated plate SAHs were presented. The effect of mass flow rates of air on pressure drop, thermal and thermo-hydraulic efficiencies of the flat and v-corrugated plate SAHs were also investigated. The results showed that the double pass v-corrugated plate SAH was 11–14% more efficient compared to the double pass flat plate SAH. It was indicated that the peak values of the thermo-hydraulic efficiencies of the flat and v-corrugated plate SAHs were obtained when the mass flow rate of the flowing air was 0.02 kg/s. As given in their earlier study [96], the thermo-hydraulic efficiency of the DPVCPSAH was 14% higher than that of the DPFPSAH.

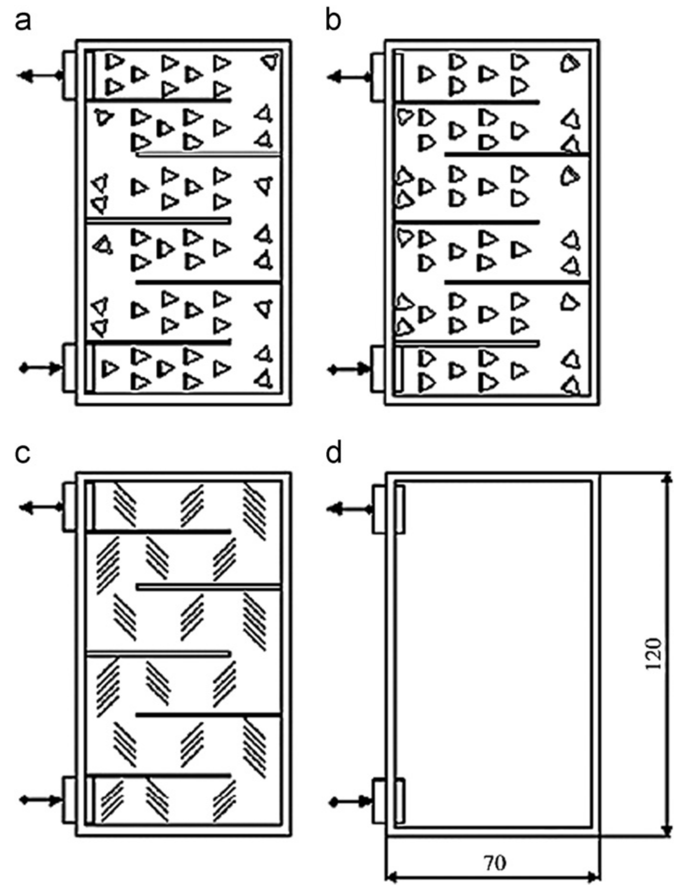

Fig. 22. Schematic views of absorber plates: (a) with the triangular type obstacles, (b) with leaf type obtacles, (c) with rectangular type obstacles, and (d) without obstacles [97].

Akpinar and Koçyiğit [97] experimentally investigated the performance analysis of a new flat-plate SAH with several obstacles (Types I–III) and without obstacles (Type IV) as given in Fig. 22 as given in Ref. [97]. Experiments were performed for two air mass flow rates of 0.0074 and 0.0052 kg/s. The first and second laws of efficiencies were determined for SAHs and comparisons were made among them. The values of first law efficiency varied between 20% and 82%. The values of second law efficiency changed from 8.32% to 44.00%. The highest efficiency were determined for the SAH with Type II absorbent plate in flow channel duct for all operating conditions, whereas the lowest values were obtained for the SAH without obstacles (Type IV).

Chamoli et al. [98] studies include the design of double pass solar air heater, heat transfer enhancement, flow phenomenon and pressure drop in duct. This paper presents an extensive study of the research carried out on double pass solar air heater. Based on the literature review, it is concluded that most of the studies carried out on double pass solar air heater integrated with porous media and extended surfaces. Mathematical models based on energy analysis of some configurations of solar air heater have been discussed.

7. Computational studies on solar air collectors

Computational Fluid Dynamics (CFD) is an effective tool to obtain heat transfer, flow field and temperature distribution in an energy system. It can also be used to simulate air flows inside the solar air collectors.

Layek et al. [99] analyzed the effect of chamfering on heat transfer and friction characteristics of SAH having absorber plate roughened with compound turbulators as shown in Fig. 23 from Ref. [100]. These boundary conditions corresponded closely to those found in SAHs. Six roughened plates were tested by placing a 60° V-groove at the center line in between two consecutive chamfered ribs. The ribs' top were chamfered having chamfer angles of 5°, 12°, 15°, 18°, 22° and 30°, while relative roughness pitch (P/e) and relative roughness height (e/Dh) of the ribs were kept constant having values of 10 and 0.03 respectively. The flow Reynolds number of the duct varied in the range of approximately 3000–21,000, most suitable for SAH. The effects of chamfer angle on Nusselt number and friction factor were discussed and the results were compared with the square rib-grooved and smooth duct under similar flow conditions to investigate the enhancement in Nusselt number and friction factor. The conditions for the maximum enhancement of Nusselt number and friction factor were determined. It was found that the thermo-hydraulic performance of the SAH provided with such roughness was considerably enhanced. Fig. 24 illustrates the streamlines for different geometries while thermohydraulic performance (Eq. (6)) for different Reynolds numbers is indicated in Fig. 25 as in Ref. [99]. It was found that the value of performance parameter increased with increase in Reynolds number and the rate of increase of the performance parameter was very sharp for the values of Reynolds number below of about 8000.

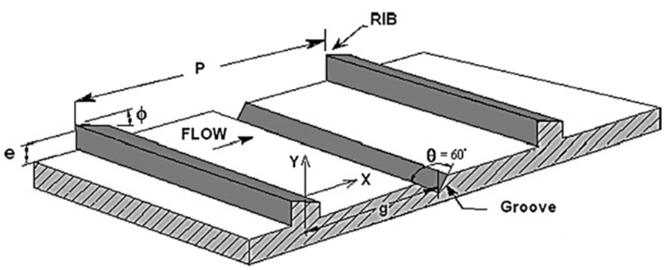

Fig. 23. Roughness geometry [99].

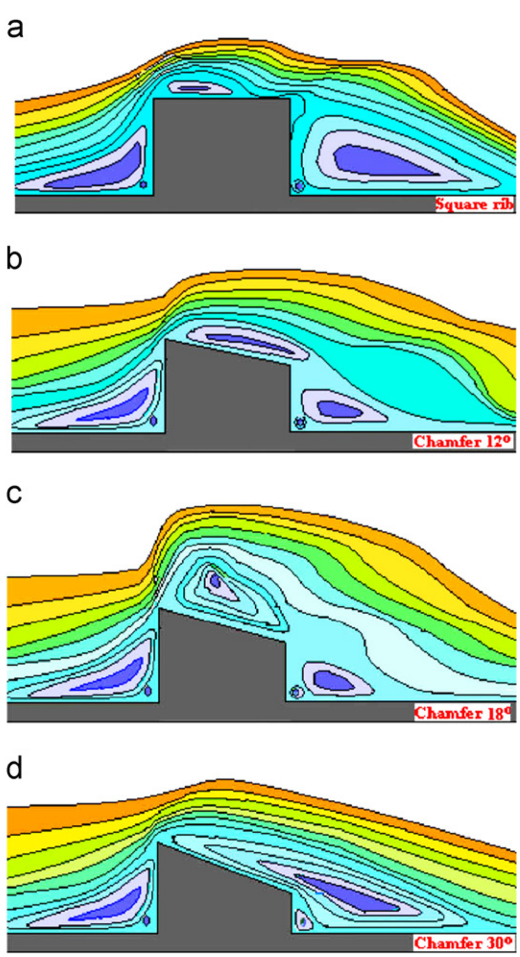

Fig. 24. (a) square rib, (b) chamfer 12°, (c) chamfer 18°, and (d) chamfer 30° [99].

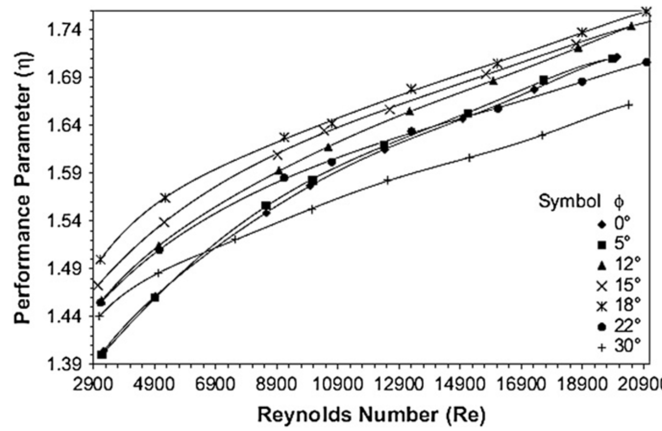

Fig. 25. Thermo-hydraulic performance parameter as a function of Reynolds number [99].

$$\eta = \frac{(Nu/Nu_s)}{(f/f_s)} \tag{6}$$

Saim et al. [100] presented a computational analysis on the turbulent flow and heat transfer in solar air collector with rectangular plate fins absorber and baffles, which were arranged on the bottom and top channel walls in a periodically staggered way. Their model is given in Fig. 26. They made a numerical analysis using finite volume methods. They used low Reynolds number k–ε model as turbulence model. The velocity and pressure terms of momentum equations are solved by the SIMPLE algorithm. They found that increasing the Reynolds number will increase the efficiency of the solar panel which is an expected result.

Fig. 26 presents the upward type SAH under consideration. The physical domain was between two parallel plates [100]. The outer surface of the top wall of the channel was uniformly heated while the outer surface of the bottom wall was thermally insulated.

The temperature contours in the solar collector with baffles and fins are plotted in Fig. 27 as given in Ref. [100]. The plot shows that the fluid temperature in the vortex region was significantly high as compared to that in the same region of no baffle region. In the region downstream of the two baffles, recirculation cells with low temperature were observed. In the regions between the tip of the fins and the channel wall, the temperature increased. Due to the changes in the flow direction produced by the presence of the singularity of obstacles, the highest temperature value appeared behind the lower channel wall with an acceleration process that starts just after the first fin and the second baffle.

Ammari [101] developed a mathematical model for computing the thermal performance of a single pass flat-plate solar air collector. The influence of the addition of the metal slats on the efficiency of the solar collector was studied. The effects of volume air flow rate, collector length, and spacing between the absorber and bottom plates on the thermal performance of the present SAH

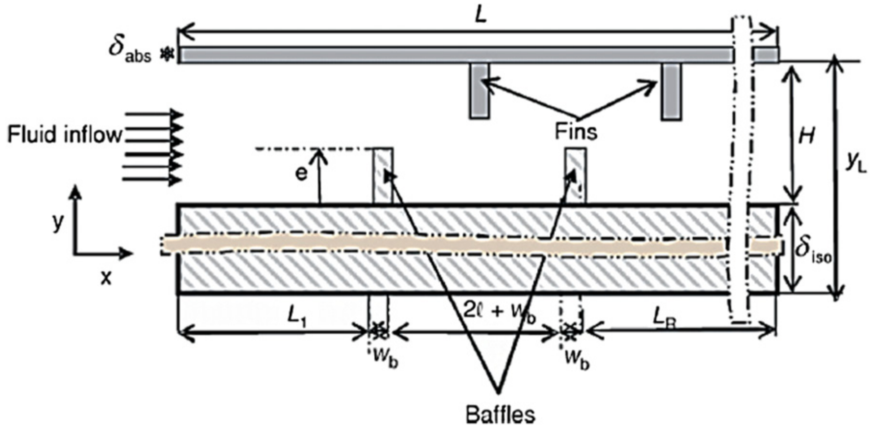

Fig. 26. Schematic model of a solar air heater proposed by Saim et al. [100].

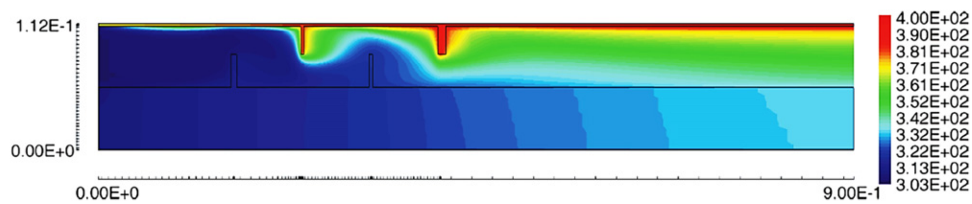

Fig. 27. Temperature (K) distribution in the solar collector (m=20 kg/h, L/B=3/2, I0=1043 W/m^2, R=16 cm) [100].

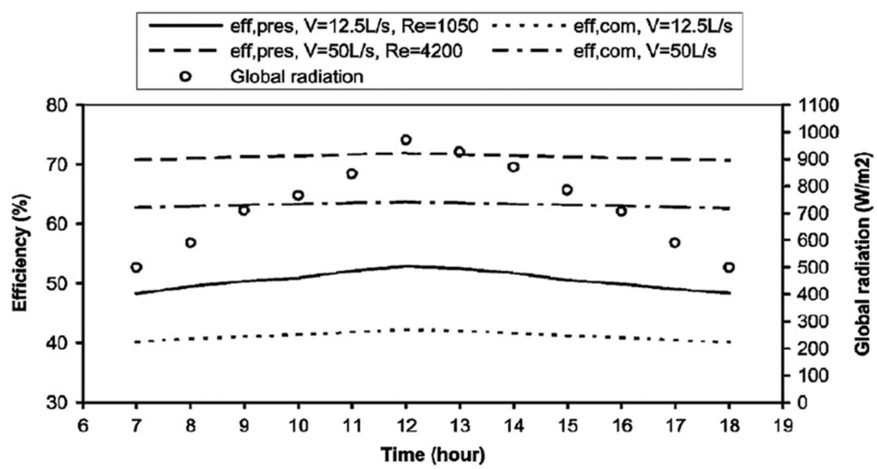

Fig. 28. Comparison of efficiency between present and commonn type solar air heaters [101].

were investigated. Furthermore, a numerical comparison of the present design with the most common type of SAHs was conducted. The results of the comparison indicated that better thermal performance was obtained by the modified system, as given in Fig. 28 as shown in Ref. [101] Karmare [114] made a computational analysis of different types of solar collectors.

8. Energy and exergy analysis of solar air collectors

8.1. Energy analysis

The theoretical model employed for the study of the solar collector that operates in unsteady state is made using a thermal

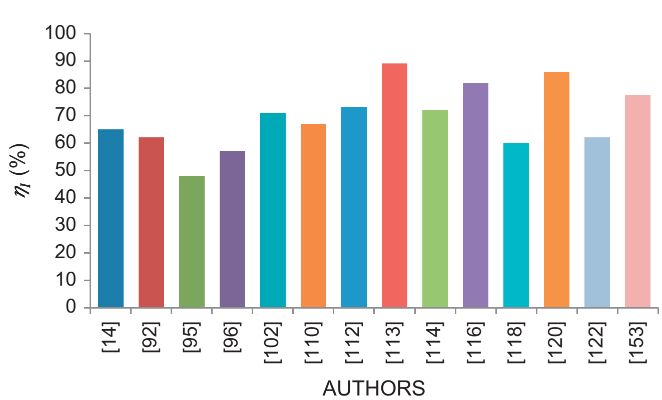

Fig. 29. Variation of energy efficiency by various investigators.

Table 2
List of some earlier works.

Authors	Method	Flow	Glass	Flow rate	Dimensions (L, B) (m)		System	Remarks	η_{I} (%)	η_{II} (%)
Esen [14]	E	Double pass flow	Single glass cover	0.015 kg/s	1.25		Experimental energy and exergy analysis of a double-flow solar air heater having different obstacles on absorber plates	Test results always yield higher efficiency values for Type III than for Type I (without obstacles) flat plate collector. The obstacles ensure a good air flow over and under the absorber plates, create the turbulence, and reduce the dead zones in the collector.	$\boldsymbol{\eta}=\mathbf{65}$, State II, Type III, 0.025 kg/s	$\boldsymbol{\eta}=\mathbf{60.97}$, State II, Type III, 0.025 kg/s
				0.02 kg/s	0.8					
				0.025 kg/s						
Yeh and Ho [92]	T	Single (recycle) pass flow	Single glass cover	0.01 kg/s	0.6		Effect of external recycle on the performance of flat-plate solar air heaters with internal fins attached	It is found that considerable improvement in collector efficiency is obtainable if the operation is carried out with an external recycle, where the desirable effect overcomes the undesirable effect. The enhancement increases with increasing reflux ratio, especially for operating at lower air flow rate with higher inlet air temperature.	$\boldsymbol{\eta}=\mathbf{61.11}$, $T=288$ K, $R=5$, $\dot{m}=0.02$	
				0.015 kg/s	0.6					
				0.02 kg/s						
Yeh and Ho [91]	T	Single pass flow	Double glass cover	0.01 kg/s	0.6		Downward-type solar air heaters with internal recycle	It is found that considerable improvement in collector efficiency is obtainable if the operation is carried out with an internal recycle, where the desirable effect of increasing fluid velocity to decrease the heat transfer resistance compensates for the undesirable effect of decreasing the driving force (temperature difference) of heat transfer, due to the remixing effect at the inlet by recycle operation	$\boldsymbol{\eta}=\mathbf{62}$, $T_{fi}=298$ K, $\dot{m}=0.02$	
				0.015 kg/s	0.6					
				0.02 kg/s						
Yeh et al. [93]	T	Single pass flow	Double glass cover	–	L	B	Effect of collector aspect ratio on the collector efficiency of upward type baffled solar air heaters	It is obtained same results with flat plate solar air heaters without fins and baffles. Although the collector efficiency of baffled solar air heaters is larger than that of flat plate heaters without fins and baffles, the improvement of collector efficiency by increasing the collector aspect ratio is the reverse.	$\boldsymbol{\eta}=\mathbf{68}$, $L=1.8$ for $B=0.3$	
					1.8	0.3				
					0.9	0.6				
					0.6	0.9				
					0.3	1.8				
El-Sabii and Al-Snani [94]	T	Single pass flow	Double glass cover	0.00117 kg/s	1		Effect of selective coating on thermal performance of flat plate solar air heaters	To improve the heater performance, effect of using absorber plates coated with various selective coating materials on the heater performance was also investigated. The best performance was achieved using nickel–tin as a selective coating material with a daily average of the instantaneous efficiency of 0.46.	$\boldsymbol{\eta}=\mathbf{48}$, Ni–Sn for 0.005 kg/s	
				0.005 kg/s	1					
Ramadan et al. [95]	E–T	Double (countrary) pass flow	Double pass flow	0.0105	1		Thermal performance of a packed bed double-pass solar air heater	Limestone and gravel were used as packed bed materials. The thermo-hydraulic efficiency η_{TH} was found to increase with increasing $\dot{m}_f$ until a typical value of 0.05 kg/s beyond which the increase in η_{TH} becomes insignificant. To validate the proposed mathematical model, comparisons between experimental and theoretical results showed that good agreement was achieved.	The daily average values of η_{TH} are obtained as 57.2% with gravel	
				0.02	1					
				0.04…0.0.14						
Akpinar and Koçyiğit [97]	E	Single pass flow	Single glass cover	0.0074 kg/s	1.2		Experimental investigation of thermal performance of solar air heater having different obstacles on absorber plates	The optimal value of efficiency was determined for the solar air heater with Type II absorbent plate in flow channel duct for all operating conditions and the collector supplied with obstacles appears significantly better than that without obstacles	Type II, 0.074 kg/s, $\boldsymbol{\eta}=\mathbf{82}$	
				0.0052 kg/s	0.7					

Ammari [101]	T	Single pass flow	Single glass cover	12.5 L/s	6	A mathematical model of thermal performance of a solar air heater with slats	A numerical comparison of the present design with the most common type of solar air heaters is conducted. The results of the comparison have indicated that better thermal performance was obtained by the modified system	$V=50$ L/s, $Re=4200$, $\boldsymbol{\eta \cong 71}$	
Alta et al. [107]	E	Single pass flow	Doubleand single glass cover	125 L/s $25\cdots5$ m^3/m^2h	1 0.63	Experimental investigation of three different solar air heaters: Energy and exergy analyses	Based on the energy and exergy output rates, heater with double glass covers and fins (Type II) is more effective and the difference between the input and output air temperature is higher than of the others.	$30\cdots100$ m^3/m^2 h, $\eta_I=39.05$	$0\cdots100$ m^3/m^2 h, $\eta_{II}=0.834$
El-Sabii et al. [109]	E–T	Double pass flow	Double glass cover	$0\cdots100$ 0–0.06	0.315	Thermal performance investigation of double pass-finned plate solar air heater	The results showed that the double pass v-corrugated plate solar air heater is 9.3–11.9% more efficient compared to the double pass-finned plate solar air heater.	$\boldsymbol{\eta \cong 67}$, 0.05 kg/s v-corrugated	$\boldsymbol{\eta = 57.7}$ 0.0225 kg/s v-corrugated
El-Sabii et al. [110]	E–T	Double pass flow	Double glass cover	0–0.06		Investigation of thermal performance of-double pass-flat and v-corrugated plate solar air heaters	The results showed that the double pass v-corrugated plate solar air heater is 11–14% more efficient compared to the double pass flat plate solar air heater. It is also indicated that the peak values of the thermo-hydraulic efficiencies of the flat and v-corrugated plate solar air heaters are obtained when the mass flow rate of the flowing air is 0.02 kg/s.	$\boldsymbol{\eta = 67}$, 0.05 kg/s v-corrugated	$\boldsymbol{\eta = 57}$ v-corrugated
Gao et al. [111]	E–T	Single pass flow	Single glass cover	0.1 kg/m^2 s	2	Analytical and experimental studies on the thermal performance of cross-corrugated and flat-plate solar air heaters	All the analytical and experimental results show that, although the thermal performance of the type 2 heater is just slightly superior to that of the type 1 heater, both of these cross-corrugated solar air-heaters have a much superior thermal performances to that of the flat-plate one.	Exp. Case 4, Type 2, $\boldsymbol{\eta = 73.18}$ analytical case 4, type 2 $\boldsymbol{\eta \cong 75}$	
Naphon [112]	T	Double pass flow (counter)	Single glass cover	Max. 0.1 kg/s	1 2.4	Effect of porous media on the performance of the double-pass flat plate solar air heater	The results obtained from the model are validated by comparison with experimental data of previous researchers. There is reasonable agreement between the present model and experiment.	$\boldsymbol{\eta \cong 89}$	
Ozgen et al. [113]	E	Double pass flow	Single glass cover	0.03 kg/s	1.2	Experimental investigation of thermal performance of a double-flow solar air heater having aluminum cans	In the first type (Type I), cans had been staggered as zigzag on absorber plate, while in Type II they were arranged in order. Type III is a flat plate (without cans). Also, comparison between the thermal efficiency of the SAH tested in this study with the ones reported in the literature had been presented, and a good agreement had been found.	Type I, 0.05 kg/s, $\boldsymbol{\eta \cong 72}$	
Akpinar and Koçyiğit [115]	E	Single pass flow	Single glass cover	0.05 kg/s 0.0074 kg/s	1.20 m	Energy and exergy analysis of a new flat-plate solar air heater having different obstacles on absorber plates	The highest efficiency were determined for the SAH with Type II absorbent plate in flow channel duct for all operating conditions, whereas the lowest values were obtained for the SAH without obstacles (Type IV).	Type II, 0.0074 kg/s, $\boldsymbol{\eta = 82}$	Type II, 0.0074 kg/s, $\boldsymbol{\eta = 44}$
Omojaro and Aldabbagh [116]	*E*	Single and double pass flow	Single glass cover	0.0052 kg/s 0.012 kg/s	0.7 m 1.5 m	Experimental performance of single and double pass solar air heater with fins and steel wire mesh as absorber	Maximum efficiency obtained for the single and double pass air heater was 59.62% and 63.74% respectively for air mass flow rate of 0.038 kg/s.	0.038 kg/s, $\boldsymbol{\eta_{si}=59.62}$, $\boldsymbol{\eta_d=63.74}$	
Assari et al. [117]	E–T	Single pass flow	Single glass cover	0.038 kg/s Between 0.02 and 0.14 kg/s	1 m 1.94	Experimental and theoretical investigation of a dual purpose solar collector	High temperature and high performance can be obtained using dual purpose solar collector (DPSC) compared to single water or air collector.	$\boldsymbol{\eta = 60}$, 0.02 kg/s rectangular fin	
Yang et al. [118]	E	Single pass flow	Single glass cover		0.94 2	Experimental analysis on thermal performance of a solar air collector with a single pass	Based on the results, decreasing the heat transfer resistance in the air flow channel had the most significant effect on thermal efficiency enhancement.	$\boldsymbol{\eta = 38.3}$ for type E	
El-khawajah et al. [119]	E	Single pass flow	Double glass cover		1 1.5 m	The effect of using transverse fins on a double		$\boldsymbol{\eta = 85.9}$ for 6 fins to 0.042 kg/s	

Table 2 (*continued*)

Authors	Method	Flow	Glass	Flow rate	Dimensions (*L*, *B*) (m)	System	Remarks	η_I (%)	η_{II} (%)
				Between 0.0121 and 0.042 kg/s.	1 m	pass flow solar air heater using wire mesh as an absorber	The thermal efficiency of the 6 fins SAH was compared with some of the reported ones. The thermal efficiency was higher compared to the other models.		
Gill et al. [120]	E	Single pass flow	Both single and double glass cover	0.011, 0.014, 0.017 and 0.020 m^3/s per m^2	2.06 m 0.72 m (for single glass cover) 2.16 m 0.82 m (for double glass cover)	Low cost solar air heater	Two low cost solar air heaters viz. single glazed and double glazed were designed, fabricated and tested. The maximum efficiency of single glazed, double glazed and packed bed solar air heater was 37.45%, 24.07% and 66.23%, respectively.	For summer ***η* =66.23** and for winter ***η* =71.68**	
Yeh [121]	T	Double pas flow (recycle)	Double glass cover	0.01, 0.015 and 0.02 kg/s	0.6 m 0.6 m	Upward-type flat-plate solar air heaters attached with fins and operating by an internal recycling for improved performance.	The effect of internal recycle on the collector efficiency in upward-type flat-plate solar air heaters attached with fins was investigated theoretically. It was found that more than 100% of improvement in the collector efficiency was obtained by recycling operation.	***η* ≅ 62** for 0.02 kg/s	
Bayrak [152]	E	Single	Single	0.016 and 0.025 kg/s	1.2 m 0.7 m	Aluminium foam located	Fins with 6 mm gives better result than that of 10 mm.	**0.78**	0.52

energy balance [14]:

$$[\text{Accumulated energy}]+[\text{energy gain}]=[\text{absorbed energy}]-[\text{lost energy}] \tag{7}$$

for each term of Eq. (7) the following expressions are formulated:

$$[\text{Accumulated energy}]=M_pC_p\left(dT_{p,ave}/dT\right) \tag{8}$$

$$[\text{Energy gain}]=\dot{m}C_p(T_{out}-T_{in}) \tag{9}$$

$$[\text{Absorbed energy}]=\eta_o IA_c \tag{10}$$

$$[\text{Lost energy}]=U_c\left(T_{p,ave}-T_e\right)A_c \tag{11}$$

By combining Eqs. (8)–(11), the thermal energy balance equation necessary to describe the solar collector functioning is obtained:

$$M_pC_p\left(dT_{p,ave}/dT\right)+\dot{m}C_p(T_{out}-T_{in})=\eta_o IA_c-U_c\left(T_{p,ave}-T_e\right)A_c \tag{12}$$

The optical yield (η_o) and the energy loss coefficient (U_c) are the parameters that characterize the behavior of the solar collector. Note that A_c represents the fraction of the solar radiation absorbed by the plate and depends mainly on transmittance of the transparent covers and on the absorbance of the plate [14]. The energy loss coefficient includes the losses by the upper cover, the laterals, and the bottom of the collector. The upper cover losses prevail over the others, depending to a large extent on the temperature and emissivity of the absorbent bed, and besides, on the convective effect of the wind on the upper cover. The thermal efficiency of the solar collectors (η_I) is defined as the ratio between the energy gain and the solar radiation incident on the collector plane [9,14,102]:

$$\eta_I=\frac{\dot{m}C_p\left(T_{a,out}-T_{a,in}\right)}{(IA_c)} \tag{13}$$

Fig. 29 illustrates the energy efficiency performed by different authors. As seen in the figure, the maximum efficiency is obtained by Naphon [108].

8.2. Exergy analysis

To write the exergy equations in solar air collector systems, some assumptions made are as follows [9,14,102,103]:

(i) steady state, steady flow operation,
(ii) negligible potential and kinetic energy effects and no chemical or nuclear reactions,
(iii) air is an ideal gas with a constant specific heat, and its humidity content is ignored,
(iv) the directions of heat transfer to the system and work transfer from the system are positive.

The mass balance equation can be expressed in the rate form as

$$\sum \dot{m}_{in}=\sum \dot{m}_{out} \tag{14}$$

where $\dot{m}$ is the mass flow rate, and the subscript *in* stands for inlet and *out* for outlet. If the effects due to the kinetic and potential energy changes are neglected, the general energy and exergy balances can be expressed in rate form as given below [9,14,102,103]:

$$\sum \dot{E}_{in}=\sum \dot{E}_{out} \tag{15}$$

$$\sum \dot{E}x_{in}-\sum \dot{E}x_{out}=\sum \dot{E}x_{dest} \tag{16a}$$

or

$$\dot{E}x_{dest}-\dot{E}xX_{work}+\dot{E}x_{mass,in}-\dot{E}x_{mass,out}=\dot{E}x_{dest} \tag{16b}$$

Using Eq. (16b) the rate form of the general exergy balance can be expressed as follows:

$$\sum\left(1-\frac{T_e}{T_s}\right)\dot{Q}_s-\dot{W}+\sum\dot{m}_{in}\psi_{in}=\dot{E}x_{dest} \tag{17}$$

Where

$$\psi_{in}=(h_{in}-h_e)-T_e(S_{in}-S_e) \tag{18}$$

$$\psi_{out}=(h_{out}-h_e)-T_e(S_{out}-S_e) \tag{19}$$

If Eqs. (18) and (19), are substituted in Eq. (17), it is arranged as below:

$$\left(1-\frac{T_e}{T_s}\right)\dot{Q}_s-\dot{m}\left[(h_{out}-h_{in})-T_e(S_{out}-S_{in})\right]=\dot{E}x_{dest} \tag{20}$$

where $\dot{Q}_s$ is the solar energy absorbed by the collector absorber surface and it is evaluated with the expression given below [9,14,102]:

$$\dot{Q}_s=I(\tau\alpha)A_c \tag{21}$$

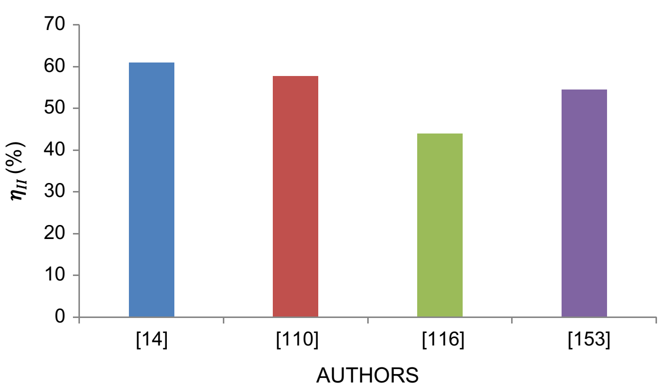

Fig. 30. Variation of exergy efficiency by various investigators.

The changes in the enthalpy and the entropy of the air at the collector are expressed by [9,14,102,103]

$$\Delta h=h_{out}-h_{in}=C_p\left(T_{f,out}-T_{f,in}\right) \tag{22}$$

$$\Delta s=s_{out}-s_{in}=C_p\ln\frac{T_{f,out}}{T_{f,in}}-R\ln\frac{P_{out}}{P_{in}} \tag{23}$$

By substituting Eqs. (21)–(23), into Eq. (20) the equation below can be derived [9,14,102]:

$$\left(1-\frac{T_e}{T_s}\right)I(\tau\alpha)A_c-\dot{m}C_p\left(T_{f,out}-T_{f,in}\right)+\dot{m}C_pT_e\ln\frac{T_{f,out}}{T_{f,in}}-\dot{m}RT_e\ln\frac{P_{out}}{P_{in}}=\dot{E}x_{dest} \tag{24}$$

The exergy destruction or the irreversibility may be expressed as follows [9,14,102]:

$$\dot{E}x_{dest}=T_e\dot{S}_{gen} \tag{25}$$

The exergy efficiency of a solar collector system can be calculated in terms of the net output exergy of the system or exergy destructions in the system. The exergy efficiency of SAH system has been evaluated in terms of the net output exergy of the system. The second law efficiency is calculated as follows [103]:

$$\eta_{II}=\frac{\dot{E}x_{out}}{\dot{E}x_{in}}=\frac{\dot{m}[h_{out}-h_{in}-T_e(S_{out}-S_{in})]}{(1-(T_e/T_s))\dot{Q}_s} \tag{26}$$

When dealing with the exergy of a process component, the difference between exergy losses and destruction should be noted. Exergy losses consist of exergy flowing to the surroundings whereas exergy destruction indicates the loss of exergy within the system boundary due to irreversibility [100]. Phrasing it another way, the exergy destruction is the actual change in exergy for the irreversible process minus the change in exergy that would have occurred if the process had been reversible.

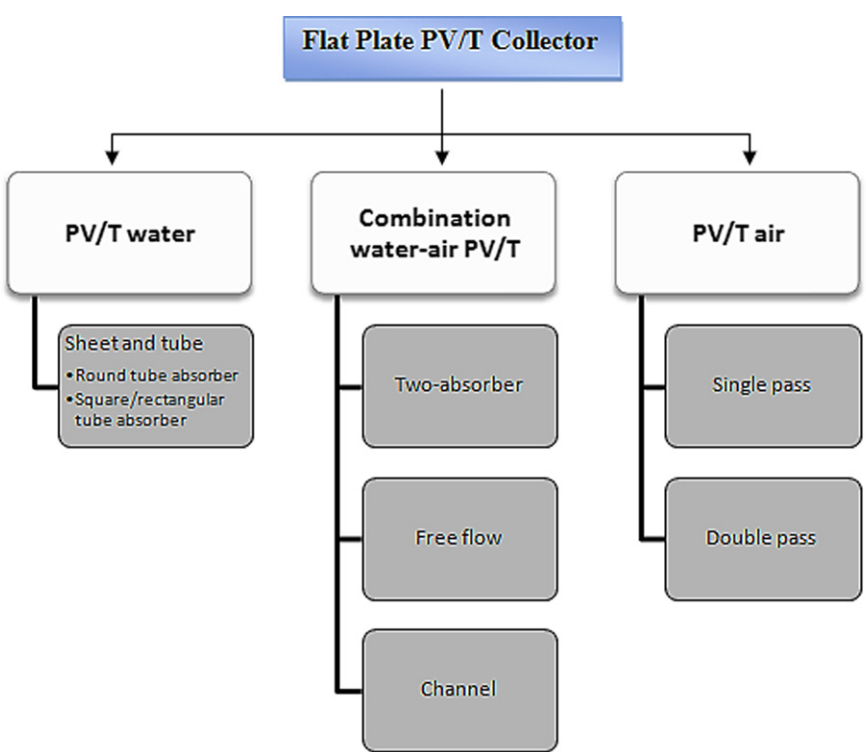

Fig. 31. Flat plate PV/T collector classification (modified from Ref. [122]).

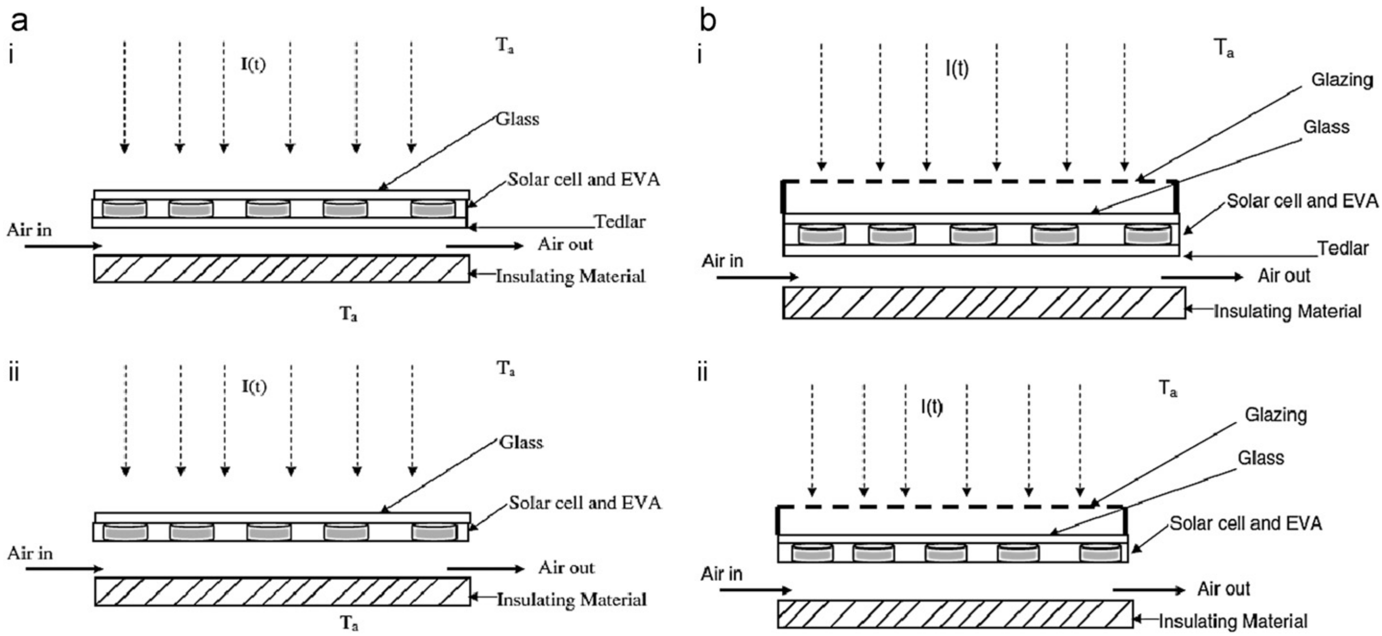

Fig. 32. Cross-section of unglazed PV/T air (a): (i) with tedlar and (ii) without tedlar and (b): (i) glazed with tedlar and (ii) without tedlar [123].

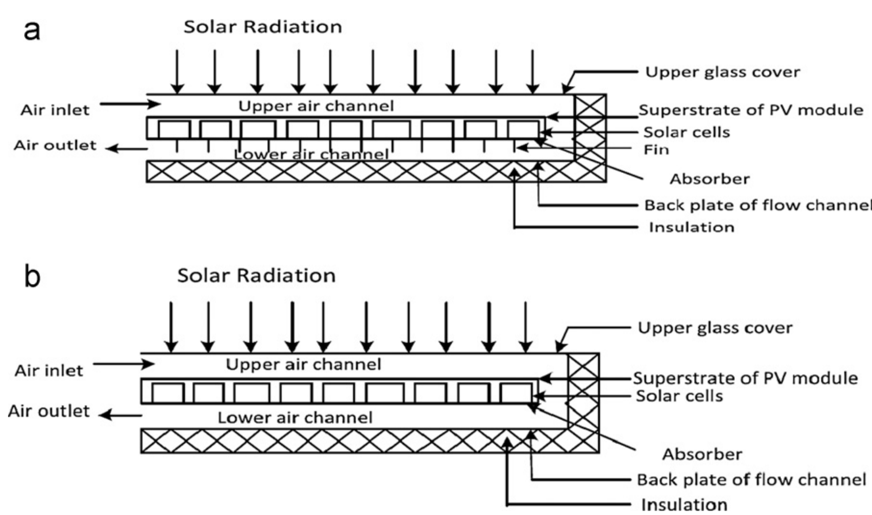

Fig. 33. The directions of air movement in both the channels along with the depths of the upper and lower channels are shown in the supplement diagrams of Fig. 1(a) and (b) from Ref. [124].

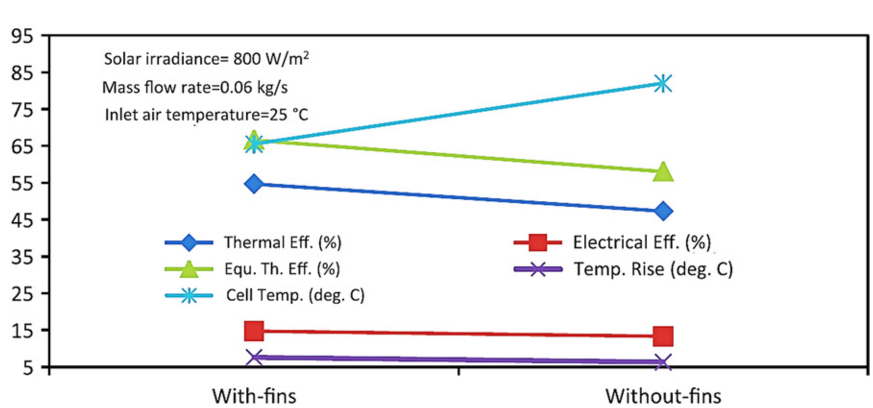

Fig. 34. The thermal efficiency, electrical efficiency, total equivalent thermal efficiency and the rise in the air and cell temperatures for a solar PV/T system with and without fins [124].

The exergy destruction due to the irreversibility generates when chemical reaction, heat transfer, pressure drop and mixing proceed in the process [104,105].

The dimensionless exergy destruction or loss is the result of dividing Eq. (25) by the energy gain value of Eq. (9) [103]

$$EX_D = \frac{\dot{E}X_{dest}}{\dot{Q}_c} \tag{27}$$

Van Gool [106] has also proposed that maximum improvement in the exergy efficiency for a process or system is obviously achieved when the exergy loss or irreversibility $Ex_{in} - Ex_{out}$ is minimized. Consequently, he suggested that it is useful to employ the concept of an exergetic "improvement potential" when analyzing different processes or sectors of the economy. This improvement potential in the rate form is denoted by Refs. [106,115]

$$I\dot{P} = (1-\eta_{II})(\dot{E}x_{in} - \dot{E}x_{out}) \tag{28}$$

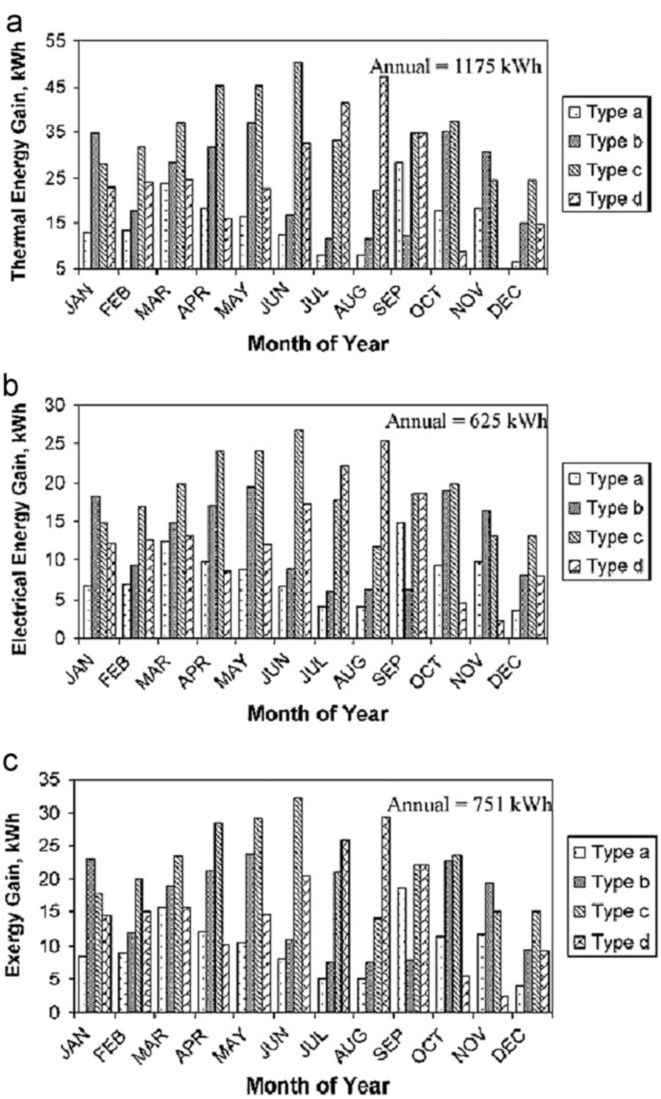

Fig. 35. (a) Monthly variation of thermal energy gain by considering a, b, c, d type weather conditions of New Delhi. (b) Monthly variation of electrical energy gain by considering a, b, c, d type weather conditions of New Delhi. (c) Monthly variation of exergy gain by considering a, b, c, d type weather conditions of New Delhi [143].

All physical properties of air were selected according to the following bulk mean temperature:

$$\Delta T_m = \frac{(T_{in} - T_{out})}{2} \tag{29}$$

In this context, Alta et al. [107] compared three different types of designed flat-plate SAHs, two having fins (Types II and III) and the other without fins (Type I), one of the heater with a fin had single glass cover (Type III) and the others had double glass covers (Types I and II). The energy and exergy output rates of the SAHs were evaluated for various air flow rates (25, 50 and 100 m^3/m^2 h), tilt angle (0°, 15° and 30°) and temperature conditions versus time. The efficiencies of the finned collectors (collector Types II and III) is higher than that of the collector without fin (Type I). The largest irreversibility occurs at Type I (without fins) in which collector efficiency is smallest, and the lowest irreversibility was found at Type II (with fins). Results for energy and exergy are shown in Table 2. As seen from the table, mean highest exergy efficiency (0.8340%) and the mean lowest exergy loss (99.166%) for Type II were found at air flow rate of 100 m^3/m^2 h and 0° tilt angle.

Ozturk and Demirel [108] made an experimental investigation of the thermal performance of a SAH having its flow channel packed with Raschig rings. They observed that the energy and exergy efficiencies of the packed-bed SAH increased as the outlet temperature of heat transfer fluid increased. Akpinar and Koçyiğit [115] experimentally studied the new flat-plat SAH with several obstacles and without obstacles for different air flow rate. They performed the first and second laws of efficiencies for SAHs and comparisons were made among them. They indicated that the values of first law efficiency varied between 20% and 82% and second law efficiency changed from 8.32% to 44.00%.

Bayrak [152] made an experimental analysis of solar air heater with porous obstacles. In this experimental work, porous baffles with different thicknesses are used as a passive element inside the SAH. Closed-cell aluminum foams are chosen as porous materials. These porous materials are 6 mm and 10 mm in thickness and have a surface area of 50 cm^2. They were placed sequent and staggered into the SAH. Six SAHs were tested at two air mass flow rates of 0.016 and 0.025 kg/s. The performances of the heaters were assessed using energy and exergy analysis methods. The highest collector efficiency and air temperature rise were achieved by SAHs with a thickness of 6 mm and an air mass flow rate of 0.025 kg/s, whereas the lowest values were obtained for the SAH without obstacles.

Fig. 30 shows the energy efficiency performed by different authors. As seen from the figure, the maximum efficiency is obtained by Esen [14].

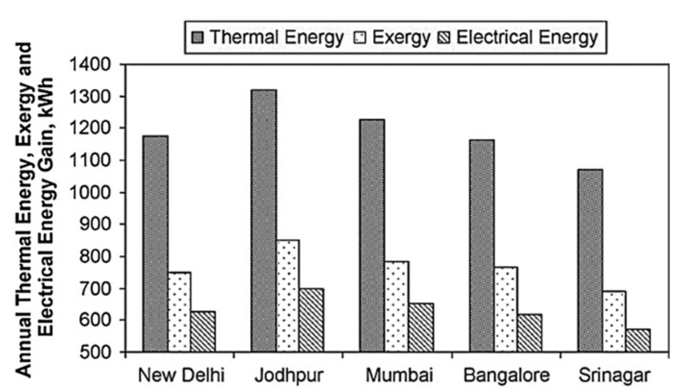

Fig. 36. Annual gain in energy, exergy and electrical energy for five different cities of India by considering a, b, c, d type weather conditions [143].

9. Recent advances in flat plate photovoltaic/thermal (PV/T) solar collectors

Flat plate photovoltaic/thermal (PV/T) solar collector produces both thermal energy and electricity simultaneously. Flat plate photovoltaic/thermal (PV/T) solar collector produces both thermal energy and electricity simultaneously. The state-of-the-art on flat plate PV/T collector classification, design and performance evaluation of water, air and combination of water and/or air based were presented Ibrahim et al. [122]. Different design features and performance of flat plate PV/T solar collectors were compared and discussed. Future research and development (R&D) works were proposed.

In conclusion, the PV/T can be improved further based on few suggestions, such as:

- New design of absorber collector to improve efficiency of the PV.
- Replacing the roofing material with new material that will increase the efficiency of the system and at the same time

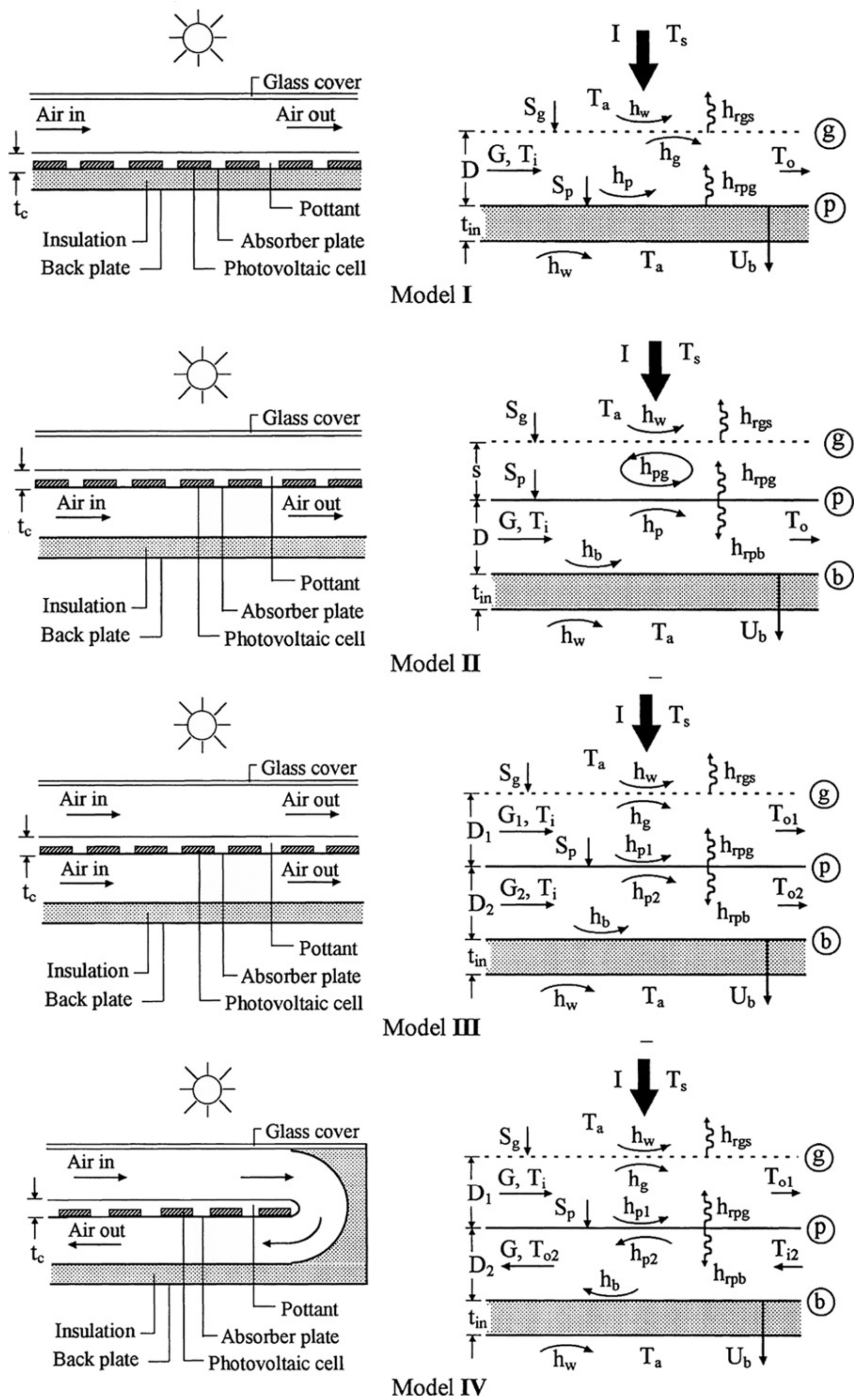

Fig. 37. Schematics of the various PV/T models along with heat transfer coefficients [144].

reduces the payback period—attractive in case the available roof surface is limited.
- Payback—proposed system that gain pay back in less than 10 years.
- Production and installation cost—new method to integrate the systems into one product with value added production.
- Sustainable energy—ensure that the energy produced by the system is sustainable with zero CO_2 emissions.
- Esthetics—integration rather than "bolt on roof" gives better architectural look.

Classification of PV/T collectors is presented in Fig. 31 as given [122]. Tiwari and Sodha [123] found that the glazed hybrid PV/T without tedlar gave the best performance compared to all configurations being evaluated in Fig. 32.

Kumar and Rosen [124] studied the performance evaluation of a double pass PV/T SAH with and without fins. They provided useful insights into the thermal and electrical behavior of a double-pass air heater with vertical fins in the lower air channels and the relevance of fins with absorber surface in the overall performance enhancement of PV/T collectors. The model is shown in Fig. 33 and efficiencies are shown in Fig. 34. Tonui and Tripanagnostopoulos [125] and Sukamongkol et al. [126] investigated the thermal and electricity production performance for three types of collectors. Then, Tonui and Tripanagnostopoulos [127,128] made similar analysis for 6 different collectors. Other studies related with PV/T collectors can be found in Refs. [129–142].

10. Energy and exergy analysis of PV/T air collectors connected in series

Energy and exergy analysis of PV/T air collectors connected in series have been studied by different authors. These analyses are complex due to complex structure of the collectors. In this context, Dubey et al. [143] showed the detailed analysis of energy, exergy and electrical energy by varying the number of collectors and air velocity considering four weather conditions (a, b, c and d type) and five different cities (New Delhi, Bangalore, Mumbai, Srinagar, and Jodhpur) of India. It was found that the collectors fully covered by PV module and air flows below the absorber plate gave better results in terms of thermal energy, electrical energy and exergy gain as seen from Figs. 35 and 36. Hegazy [144] made an extensive investigation of the thermal, electrical, hydraulic and overall performances of flat plate photovoltaic/thermal (PV/T) air collectors. Four popular designs were considered with the air flowing either over the absorber (Model I) or under it (Model II) and on both sides of the absorber in a single pass (Model III) or in a double pass fashion (Model IV). The effects of air specific flow rate and the selectivity of the absorber plate and PV cells on the performances were examined. It was found that under similar operational conditions, the Model I collector had the lowest performance, while the other models exhibited comparable thermal and electrical output gains. Nevertheless, Model III collector demanded the least fan power, followed by Models IV and II. As a conclusion, the design of Case I was efficient at higher air velocity and for one collector. However, the design of Case II was efficient for lower air velocity and higher number of collectors connected in series (Figs. 37 and 38). Joshi and Tiwari [4] studied energy and exergy efficiencies of a hybrid photovoltaic–thermal (PV/T) air collector. The performance of a hybrid PV/T parallel plate air collector were investigated for four climatic conditions and then exergy efficiencies were carried out. It was observed that an instantaneous energy and exergy efficiency of PV/T air heater varied between 55–65% and 12–15%, respectively (Fig. 39). Sarhaddi et al. [145] evaluated the PV/T solar air collectors from the exergy point of view (Table 3).

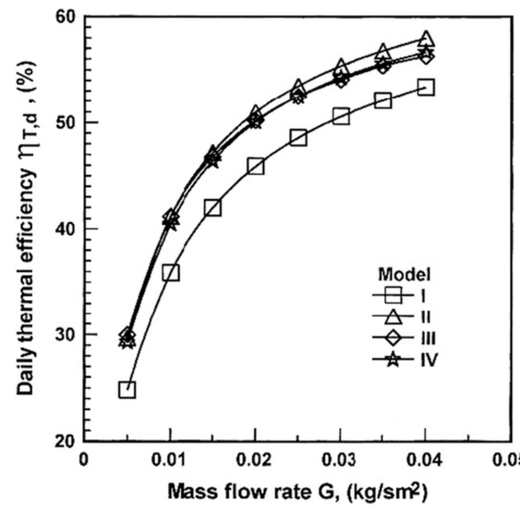

Fig. 38. Variation of daily thermal efficiency with air specific mass rate for PV/T collectors I–IV [144].

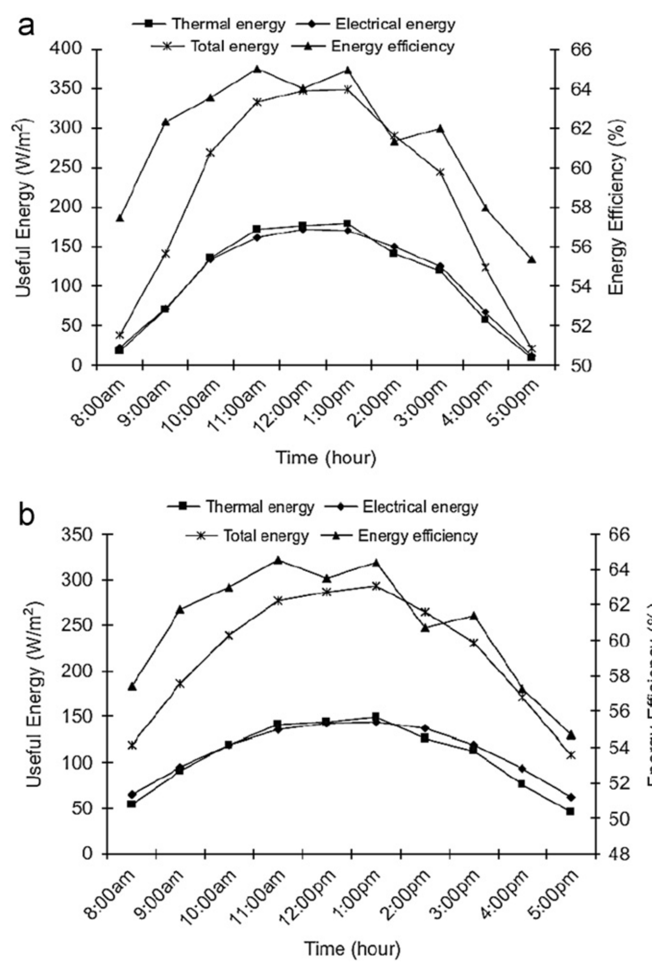

Fig. 39. (a) Electrical, thermal and total exergy and exergy efficiency for January at Srinagar. (b) Electrical, thermal and exergy and exergy efficiency for June at Srinagar [4].

Table 3
List of some studies conducted on PV/T collectors.

Investigators	Method		System	Remarks
	E (Exp.)	T (Theory)		
Tiwari and Sodha [123]	E	T	Parametric study of various configurations of hybrid PV/thermal air collector: Experimental validation of theoretical model	Numerical computations have been carried out for composite climate of New Delhi and the results for different configurations have been compared. The thermal model for unglazed PV/T air heating system has also been validated experimentally for summer climatic conditions. It is observed that glazed hybrid PV/T without tedlar gives the best performance.
Othman et al. [146]	E		Development of advanced solar assisted drying systems	The use of solar dryers will enhanced the environment, wealth creation and nation building as well as sustainable development for the country.
Garg and Adhikari [147]		T	Conventional hybrid photovoltaic/thermal (PV/T) air heating collectors: steady-state simulation	A simulation model is developed and various performance parameters are calculated for single-glass and double-glass configurations. Result are presented to show the effect of various design and operational parameters on the performance of a system. It has also been observed that for larger values of duct depth the percentage decrease in performance of the double-glass configuration is smaller than for the single-glass configuration.
Solanki et al. [148]	E	T	Indoor simulation and testing of photovoltaic thermal (PV/T) air collectors	An indoor standard test procedure has been developed for thermal and electrical testing of PV/T collectors connected in series. Comparison between experimental and theoretical results were also been carried out. The thermal and electrical efficiency of the solar heater is 42% and 8.4%, respectively.
Sarhaddi et al. [149]		T	An improved thermal and electrical model for a solar photovoltaic thermal (PV/T) air collector	It is also found that the thermal efficiency, electrical efficiency and overall energy efficiency of PV/T air collector is about 17.18%, 10.01% and 45%, respectively, for a sample climatic, operating and design parameters
Alfegi et al. [150]		T	Transient mathematical model of both side single pass photovoltaic thermal air collector	A mathematical model and solution procedure of a single pass photovoltaic thermal air collector (PVT) with Compound Parabolic Concentrator (CPC) and fins with both sides of the absorber for predicting the thermal and combined photovoltaic thermal performance of the system is presented. Results at solar irradiance of 400 W/m^2 show that the combined PV/T efficiency is increasing from 26.6% to 39.13% at mass flow rates varies from 0.0316 to 0.09 kg/s.
Alfegi et al. [151] cc	E		Experimental investigation of single pass, double duct photovoltaic thermal (PV/T) air collector with CPC and fins	An experimental investigation of a solar air heater with photovoltaic cell located at the absorber with compound parabolic collector (CPC) and fins have been developed and tested. Results at solar irradiance of 400 W/m^2 showed that the combined PV/T efficiency is increasing from 27.50% to 40.044% at mass flow rates various from 0.0316 to 0.09 kg/s

11. Conclusions

A review has been performed on experimental and numerical studies of SAHs for the last 40 years. The main conclusions, which may be drawn from the results of the present study, are listed below:

(a) Solar air collectors can be used to enhance the temperature of air used in different systems. The SAHs have become a very popular subject on which many researchers have focused in the recent years.
(b) Studies conducted mostly focused on the enhancement of heat transfer in solar air collectors by using passive heat transfer enhancement techniques.
(c) In any cases, body added (V-groove, fin etc.) SAHs have more efficiency than that of flat plate collectors.
(d) Both theoretical and experimental analyses done were much in numbers. It was also observed that Computational Fluid Dynamics (CFD) methods can be used to analyze the efficiency of SAHs systems.
(e) Energy analysis method has been used in a number of studies while works conducted on exergy analysis were very low in numbers. Energy efficiencies of solar air collectors reviewed changed between 47% and 89%.
(f) SAHs systems become more efficient when they are used for both space heating and electricity generation via PV/T systems.
(g) Exergy analysis is also an effective way to analyze the effectiveness of PV/T systems.

Efficiencies are strongly depended on the SAH material such as cover, absorber etc. Single or double pass collectors also play an important role in terms of efficiency.

Acknowledgments

The authors gratefully acknowledge the financial support provided by the Firat University Scientific Research Unit (FUBAP) under the project no. TEKF.10.01.

References

[1] Close DJ. Solar air heaters. Solar Energy 1963;7:117–29.
[2] Varun, Saini RP, Singal SK. A review on roughness geometry used in solar air heaters. Solar Energy 2007;81:1340–50.
[3] Alkilani MM, Sopian K, Sohif M, Alghol M. Output air temperature prediction in a solar air heater integrated with phase change material European. Journal of Scientific Research 2009;27:334–41.
[4] Joshi AS, Tiwari A. Energy and exergy efficiencies of a hybrid photovoltaic–thermal (PV/T) air collector. Renewable Energy 2007;32:2223–41.
[5] Vanderhulst P, Lanser H, Bergmeyer P, Foeth F, Albers R. Solar energy: small scale applications in developing countries. Amsterdam, Holland: Stichting Tool; 1990.

[6] John Perlin. Solar evolution—the history of solar energy. California Solar Center.
[7] 〈http://en.wikipedia.org/wiki/Solar_water_heating#cite_note-CSC-2〉.
[8] Pitz-Paal R. Concentrating solar technologies—the key to renewable electricity and prosee heat for a wide range of applications. In: CD-proceedings of the World Renewable Energy Congress VII (WREC 2002). 2002.
[9] Karsli S. Performance analysis of new-design solar air collectors for drying applications. Renewable Energy 2007;32:1645–60.
[10] Alvarez G, Arce J, Lira L, Heras MR. Thermal performance of an air solar collector with an absorber plate made of recyclable aluminum cans. Solar Energy 2004;77:107–13.
[11] Peng D, Zhang X, Dong H, Lv K. Performance study of a novel solar air collector. Applied Thermal Engineering 2010;30:2594–601.
[12] Garg HP, Datta G, Bhargava AK. Some studies on the flow passage for solar air heating collectors. Energy Conversion and Management 1984;24:181–4.
[13] Caner M, Gedik E, Keçebaş A. Investigation on thermal performance calculation of two type solar air collectors using artificial neural network. Expert Systems with Applications 2011;38:1668–74.
[14] Esen H. Experimental energy and exergy analysis of a double-flow solar air heater having different obstacles on absorber plates. Building and Environment 2008;43:1046–54.
[15] El-Sawi AM, Wifi AS, Younan MY, Elsayed EA, Basily BB. Application of folded sheet metal in flat bed solar air collectors. Applied Thermal Engineering 2010;30:864–71.
[16] Ucar A, Inallı M. Thermal and exergy analysis of solar air collectors with passive augmentation techniques. International Communications in Heat and Mass Transfer 2006;33:1281–90.
[17] Karim MA, Hawlader MNA. Performance evaluation of a v-groove solar air collector for drying applications. Applied Thermal Engineering 2006;26: 121–30.
[18] Moummi N, Ali SY, Moummi A, Desmons JY. Energy analysis of a solar air collector with rows of fins. Renewable Energy 2004;29:2053–64.
[19] Lalji MK, Sarviya RM, Bhagoria JL. Exergy evaluation of packed bed solar air heater. Renewable and Sustainable Energy Reviews 2012;16:6262–7.
[20] Kumar A, Saini RP, Saini JS. Heat and fluid flow characteristics of roughened solar air heater ducts—a review. Renewable Energy 2012;47:77–94.
[21] Sethi M, Varun, Thakur NS. Correlation for solar air heater duct with dimpled shape roughness elements on absorber plate. Solar Energy 2012;86: 2852–61.
[22] Karim MA, Hawlader MNA. Development of solar air collectors for drying applications. Energy Conversion and Management 2004;45:329–44.
[23] Mittal MK, Varshney L. Optimal thermohydraulic performance of a wire mesh packed solar air heater. Solar Energy 2006;80:1112–20.
[24] Hans VS, Saini RP, Saini JS. Heat transfer and friction factor correlations for a solar air heater duct roughened artificially with multiple v-ribs. Solar Energy 2010;84:898–911.
[25] Prasad SB, Saini JS, Singh KM. Investigation of heat transfer and friction characteristics of packed bed solar air heater using wire mesh as packing material. Solar Energy 2009;83:773–83.
[26] Réné T. A review of the mathematical models for predicting solar air heaters systems. Renewable and Sustainable Energy Reviews 2009;13:1734–59.
[27] Jannot Y, Coulibaly Y. The evaporative capacity as a performance index for a solar-drier air-heater. Solar Energy 1998;63:387–91.
[28] Togrul İT, Pehlivan D, Akosman C. Development and testing of a solar air-heater with conical concentrator. Renewable Energy 2004;29:263–75.
[29] Karmare SV, Tikekar AN. Experimental investigation of optimum thermohydraulic performance of solar air heaters with metal rib grits roughness. Solar Energy 2009;83:6–13.
[30] Togrul İT, Pehlivan D. Effect of packing in the airflow passage on the performance of a solar air-heater with conical concentrator. Applied Thermal Engineering 2005;25:1349–62.
[31] Gupta MK, Kaushik SC. Performance evaluation of solar air heater having expanded metal mesh as artificial roughness on absorber plate. International Journal of Thermal Sciences 2009;48:1007–16.
[32] Bansal NK. Solar air heater applications in India. Renewable Energy 1999;16: 618–23.
[33] Yamalı C, Solmuş İ. Theoretical investigation of a humidification–dehumidification desalination system configured by a double-pass flat plate solar air heater. Desalination 2007;205:163–77.
[34] Esen H, Ozgen F, Esen M, Sengur A. Modelling of a new solar air heater through least-squares support vector machines. Expert Systems with Applications 2009;36:10673–82.
[35] Bopche SB, Tandale MS. Experimental investigations on heat transfer and frictional characteristics of a turbulator roughened solar air heater duct. International Journal of Heat and Mass Transfer 2009;52:2834–48.
[36] Kumar A, Bhagoria JL, Sarviya RM. Heat transfer and friction correlations for artificially roughened solar air heater duct with discrete W-shaped ribs. Energy Conversion and Management 2009;50:2106–17.
[37] Forson FK, Nazha MAA, Rajakaruna H. Experimental and simulation studies on a single pass, double duct solar air heater. Energy Conversion and Management 2003;44:1209–27.
[38] Karwa R, Chauhan K. Performance evaluation of solar air heaters having v-down discrete rib roughness on the absorber plate. Energy 2010;35:398–409.
[39] Sun W, Ji J, He W. Influence of channel depth on the performance of solar air heaters. Energy 2010;35:4201–7.
[40] Gupta MK, Kaushik SC. Exergetic performance evaluation and parametric studies of solar air heater. Energy 2008;33:1691–702.
[41] Bhushan B, Singh R. A review on methodology of artificial roughness used in duct of solar air heaters. Energy 2010;35:202–12.
[42] Mittal MK, Varun, Saini RP, Singal SK. Effective efficiency of solar air heaters having different types of roughness elements on the absorber plate. Energy 2007;32:739–45.
[43] Gao W, Lin W, Liu T, Xia C. Analytical and experimental studies on the thermal performance of cross-corrugated and flat-plate solar air heaters. Applied Energy 2007;84:425–41.
[44] Saini RP, Verma J. Heat transfer and friction factor correlations for a duct having dimple-shape artificial roughness for solar air heaters. Energy 2008;33:1277–87.
[45] Karwa R, Karwa N, Misra R, Agarwal PC. Effect of flow maldistribution on thermal performance of a solar air heater array with subcollectors in parallel. Energy 2007;32:1260–70.
[46] Ho-Ming Y, Chii-Dong H. Effect of external recycle on the performances of flat-plate solar air heaters with internal fins attached. Renewable Energy 2009;34:1340–7.
[47] Bhagoria JL, Saini JS, Solanki SC. Heat transfer coefficient and friction factor correlations for rectangular solar air heater duct having transverse wedge shaped rib roughness on the absorber plate. Renewable Energy 2002;25: 341–69.
[48] Pramuang S, Exell RHB. The regeneration of silica gel desiccant by air from a solar heater with a compound parabolic concentrator. Renewable Energy 2007;32:173–82.
[49] Hegazy AA. Optimum channel geometry for solar air heaters of conventional design and constant flow operation. Energy Conversion and Management 1999;40:757–74.
[50] Nwosu NP. Employing exergy-optimized pin fins in the design of an absorber in a solar air heater. Energy 2010;35:571–5.
[51] Kumar S, Saini RP. CFD based performance analysis of a solar air heater duct provided with artificial roughness. Renewable Energy 2009;34:1285–91.
[52] Aldabbagh LBY, Egelioglu F, Ilkan M. Single and double pass solar air heaters with wire mesh as packing bed. Energy 2010;35:3783–7.
[53] Chaube A, Sahoo PK, Solanki SC. Analysis of heat transfer augmentation and flow characteristics due to rib roughness over absorber plate of a solar air heater. Renewable Energy 2006;31:317–31.
[54] Gupta MK, Kaushik SC. Performance evaluation of solar air heater for various artificial roughness geometries based on energy, effective and exergy efficiencies. Renewable Energy 2009;34:465–76.
[55] Naphon P. Effect of porous media on the performance of the double-pass flat plate solar air heater. International Communications in Heat and Mass Transfer 2005;32:140–50.
[56] Hatami N, Bahadorinejad M. Experimental determination of natural convection heat transfer coefficient in a vertical flat-plate solar air heater. Solar Energy 2008;82:903–10.
[57] Sahu MM, Bhagoria JL. Augmentation of heat transfer coefficient by using 90° broken transverse ribs on absorber plate of solar air heater. Renewable Energy 2005;30:2057–73.
[58] Kasayapanand N, Kiatsiriroat T. Optimized mass flux ratio of double-flow solar air heater with EHD. Energy 2007;32:1343–51.
[59] Ho CD, Yeh HM, Cheng TW, Chen TC, Wang RC. The influences of recycle on performance of baffled double-pass flat-plate solar air heaters with internal fins attached. Applied Energy 2009;86:1470–8.
[60] Wazed MA, Nukman Y, Islam MT. Design and fabrication of a cost effective solar air heater for Bangladesh. Applied Energy 2010;87:3030–6.
[61] Varun, Siddhartha, Thermal performance optimization of a flat plate solar air heater using genetic algorithm, Applied Energy, 2010;87:1793-1799.
[62] Al-Kamil MT, Al-Ghareeb AA. Effect of thermal radiation inside solar air heaters. Energy Conversion and Management 1997;38:1451–8.
[63] Layek A, Saini JS, Solanki SC. Effect of chamfering on heat transfer and friction characteristics of solar air heater having absorber plate roughened with compound turbulators. Renewable Energy 2009;34:1292–8.
[64] Jaurker AR, Saini JS, Gandhi BK. Heat transfer and friction characteristics of rectangular solar air heater duct using rib-grooved artificial roughness. Solar Energy 2006;80:895–907.
[65] Esen H, Ozgen F, Esen M, Sengur A. Artificial neural network and wavelet neural network approaches for modelling of a solar air heater. Expert Systems with Applications 2009;36:11240–8.
[66] Hegazy AA. Performance of flat plate solar air heaters with optimum channel geometry for constant/variable flow operation. Energy Conversion and Management 2000;41:401–17.
[67] Enibe SO. Thermal analysis of a natural circulation solar air heater with phase change material energy storage. Renewable Energy 2003;28: 2269–99.
[68] Toure S. Characteristic temperatures in a natural convection solar air heater. Energy Conversion and Management 2001;42:1157–68.
[69] Flores-Irigollen A, Fernández JL, Rubio-Cerda E, Poujol FT. Heat transfer dynamics in an inflatable-tunnel solar air heater. Renewable Energy 2004;29: 1367–82.
[70] Saini SK, Saini RP. Development of correlations for Nusselt number and friction factor for solar air heater with roughened duct having arc-shaped wire as artificial roughness. Solar Energy 2008;82:1118–30.

[71] Ben-Amara M, Houcine I, Guizani AA, Maalej M. Efficiency investigation of a new-design air solar plate collector used in a humidification–dehumidification desalination process. Renewable Energy 2005;30:1309–27.
[72] Karagiorgas M, Galatis K, Tsagouri M, Tsoutsos T, Botzios-Valaskakis A. Solar assisted heat pump on air collectors: a simulation tool. Solar Energy 2010;84:66–78.
[73] Romdhane BS. The air solar collectors: comparative study, introduction of baffles to favor the heat transfer. Solar Energy 2007;81:139–49.
[74] Bilgen E, Bakeka BJD. Solar collector systems to provide hot air in rural applications. Renewable Energy 2008;33:1461–8.
[75] Zhai XQ, Dai YJ, Wang RZ. Experimental investigation on air heating and natural ventilation of a solar air collector. Energy and Buildings 2005;37:373–81.
[76] Luna D, Jannot Y, Nadeau JP. An oriented-design simplified model for the efficiency of a flat plate solar air collector. Applied Thermal Engineering 2010;30:2808–14.
[77] Khedari J, Mansirisub W, Chaima S, Pratinthong N, Hirunlabh J. Field measurements of performance of roof solar collector. Energy and Buildings 2000;31:171–8.
[78] Ahmad NT. Agricultural solar air collector made from low-cost plastic packing film. Renewable Energy 2001;23:663–71.
[79] Lin W, Gao W, Liu T. A parametric study on the thermal performance of cross-corrugated solar air collectors. Applied Thermal Engineering 2006;26: 1043–53.
[80] Abdullah AH, Abou-Ziyan HZ, Ghoneim AA. Thermal performance of flat plate solar collector using various arrangements of compound honeycomb. Energy Conversion and Management 2003;44:3093–112.
[81] Abene A, Dubois V, Ray ML, Ouagued A. Study of a solar air flat plate collector: use of obstacles and application for the drying of grape. Journal of Food Engineering 2004;65:15–22.
[82] Ekechukwu OV, Norton B. Review of solar-energy drying systems III: low temperature air-heating solar collectors for crop drying applications. Energy Conversion and Management 1999;40:657–67.
[83] Román F, Nagle M, Leis H, Janjai S, Mahayothee B, Haewsungcharoen M, et al. Potential of roof-integrated solar collectors for preheating air at drying facilities in Northern Thailand, Renewable Energy, 2009;34:1661-1667.
[84] Jain D, Jain RK. Performance evaluation of an inclined multi-pass solar air heater with in-built thermal storage on deep-bed drying application. Journal of Food Engineering 2004;65:497–509.
[85] Hawlader MNA, Rahman SMA, Jahangeer KA. Performance of evaporator-collector and air collector in solar assisted heat pump dryer. Energy Conversion and Management 2008;49:1612–9.
[86] Janjai S, Tung P. Performance of a solar dryer using hot air from roof-integrated solar collectors for drying herbs and spices. Renewable Energy 2005;30:2085–95.
[87] Abene A, Dubois V, Le Ray M, Ouagued A. Study of a solar air flat plate collector: use of obstacles and application for the drying of grape. Journal of Food Engineering 2004;65:15–22.
[88] Ramani BM, Gupta A, Kumar R. Performance of a double pass solar air collector. Solar Energy 2010;84:1929–37.
[89] Sopian K, Alghoul MA, Alfegi EM, Sulaiman MY, Musa EA. Evaluation of thermal efficiency of double-pass solar collector with porous–nonporous media. Renewable Energy 2009;34:640–5.
[90] Ho CD, Yeh HM, Chen TC. Collector efficiency of upward-type double-pass solar air heaters with fins attached. International Communications in Heat and Mass Transfer 2011;38:49–56.
[91] Yeh HM, Ho CD. Downward-type solar air heaters with internal recycle. Journal of the Taiwan Institute of Chemical Engineers 2011;42:286–91.
[92] Yeh Ho-Ming, Ho Chii-Dong. Solar air heaters with external recycle. Applied Thermal Engineering 2009;29:1694–701.
[93] Yeh HM, Ho CD, Lin CY. Effect of collector aspect ratio on the collector efficiency of upward type baffled solar air heaters. Energy Conversion and Management 2000;41:971–81.
[94] El-Sebaii AA, Al-Snani H. Effect of selective coating on thermal performance of flat plate solar air heaters. Energy 2010;35:1820–8.
[95] Ramadan MRI, El-Sebaii AA, Aboul-Enein S, El-Bialy E. Thermal performance of a packed bed double-pass solar air heater. Energy 2007;32:1524–35.
[96] El-Sebaii AA, Aboul-Enein S, Ramadan MRI, Shalaby SM, Moharram BM. Investigation of thermal performance of-double pass-flat and v-corrugated plate solar air heaters. Energy 2011;88:1727–39.
[97] Akpinar EK, Koçyiğit F. Experimental investigation of thermal performance of solar air heater having different obstacles on absorber plates. International Communications in Heat and Mass Transfer 2010;37:416–21.
[98] Chamoli S, Chauhan R, Thakur NS, Siani JS. A review of the performance of double pass solar air heater. Renewable and Sustainable Energy Reviews 2012;16:481–92.
[99] Layek A, Saini JS, Solanki SC. Second law optimization of a solar air heater having chamfered rib–groove roughness on absorber plate. Renewable Energy 2007;32:1967–80.
[100] Saim R, Abbouidi S, Benyouucef B. Computational analysis of transient turbulent flow and conjugate heat transfer characteristics in a solar collector panel with internal, rectangular fins and baffles. Thermal Science 2010;14:221–34.
[101] Ammari HD. A mathematical model of thermal performance of a solar air heater with slats. Renewable Energy 2003;28:1597–615.
[102] Kurtbas I, Durmus A. Efficiency and exergy analysis of a new solar air heater. Renewable Energy 2004;29:1489–501.
[103] Cengel YA, Boles MA. Thermodynamics: an engineering approach. 5th ed New York: McGraw-Hill; 2006.
[104] Chan SH, Low CF, Ding OL. Energy and exergy analysis of simple solid-oxide fuel cell (SOFC) power systems. Journal of Power Sources 2002;103:188–200.
[105] Ishihara A, Mitsushima S, Kamiya N, Ota K-i. Exergy analysis of polymer electrolyte fuel cell systems using methanol. Journal of Power Sources 2004;126(1–2):34–40.
[106] Van Gool W. Energy policy: fairly tales and factualities. Innovation and technology 1997 pp. 93–105.
[107] Alta D, Bilgili E, Ertekin C, Yaldiz O. Experimental investigation of three different solar air heaters: energy and exergy analyses. Applied Energy 2010;87: 2953–73.
[108] Ozturk HH, Demirel Y. Exergy-based performance analysis of packed-bed solar air heaters. International Journal of Energy Research 2004;28(5): 423–32.
[109] El-Sebaii AA, Aboul-Enein S, Ramadan MRI, Shalaby SM, Moharram BM. Thermal performance investigation of double pass-finned plate solar air heater. Applied Energy 2011;88:1727–39.
[110] El-Sebaii AA, Aboul-Enein S, Ramadan MRI, Shalaby SM, Moharram BM. Investigation of thermal performance of double pass-flat and v-corrugated plate solar air heaters. Energy 2011;36:1076–86.
[111] Gao W, Lin W, Lu E. Numerical study on natural convection inside the channel between the flat-plate cover and sine-wave absorber of a cross-corrugated solar air heater. Energy Conversion and Management 2000;41:145–51.
[112] Naphon P. On the performance and entropy generation of the double-pass solar air heater with longitudinal fins. Renewable Energy 2005;30: 1345–57.
[113] Ozgen F, Esen M, Esen H. Experimental investigation of thermal performance of a double-flow solar air heater having aluminium cans. Renewable Energy 2009;34:2391–8.
[114] Karmare SV, Tikekar AN. Analysis of fluid flow and heat transfer in a rib grit roughened surface solar air heater using CFD. Solar Energy 2010;84:409–17.
[115] Akpinar EK, Koçyiğit F. Energy and exergy analysis of a new flat-plate solar air heater having different obstacles on absorber plates. Applied Energy 2010;87:3438–50.
[116] Omojaro AP, Aldabbagh LBY. Experimental performance of single and double pass solar air heater with fins and steel wire mesh as absorber. Applied Energy 2010;87:3759–65.
[117] Assari MR, Tabrizi HB, Jafari I. Experimental and theoretical investigation of dual purpose solar collector. Solar Energy 2011;85:601–8.
[118] Yang M, Wang P, Yang X, Shan M. Experimental analysis on thermal performance of a solar air collector with a single pass. Building and Environment 2012;56:361–9.
[119] El-khawajah MF, Aldabbagh LBY, Egelioglu F. The effect of using transverse fins of on a double pass flow solar air heater using wire mesh as an absorber. Solar Energy 2011;85:1479–87.
[120] Gill RS, Single S, Singh PP. Low cost solar air heater. Energy Conversion and Management 2012;57:131–42.
[121] Yeh HM. Upward-type flat-plate solar air heaters attached with fins and operated by an internal recycling for improved performance. Journal of the Taiwan Institute of Chemical Engineers 2012;43:235–40.
[122] Ibrahim A, Othman MY, Ruslan MH, Mat S, Sopian K. Recent advances in flat plate photovoltaic/thermal (PV/T) solar collectors. Renewable and Sustainable Energy Reviews 2011;15:352–65.
[123] Tiwari A, Sodha MS. Parametric study of various configurations of hybrid PV/thermal air collector: experimental validation of theoretical model. Solar Energy Materials and Solar Cells 2007;91:17–28.
[124] Kumar R, Rosen MA. Performance evaluation of a double pass PV/T solar air heater with and without fins. Applied Thermal Engineering 2011;31:1402–10.
[125] Tonui JK, Tripanagnostopoulos Y. Improved PV/T solar collectors with heat extraction by forced or natural air circulation. Renewable Energy 2007;32: 623–37.
[126] Sukamongkol Y, Chungpaibulpatana S, Limmeechokchai B, Sripadungtham P. Condenser heat recovery with a PV/T air heating collector to regenerate desiccant for reducing energy use of an air conditioning room. Energy and Buildings 2010;42:315–25.
[127] Tonui JK, Tripanagnostopoulos Y. Air-cooled PV/T solar collectors with low cost performance improvements. Solar Energy 2007;81:498–511.
[128] Tonui JK, Tripanagnostopoulos Y. Performance improvement of PV/T solar collectors with natural air flow operation. Solar Energy 2008;82:1–12.
[129] Shahsavar A, Ameri M. Experimental investigation and modeling of a direct-coupled PV/T air collector. Solar Energy 2010;84:1938–58.
[130] Charalambous PG, Maidment GG, Kalogirou SA, Yiakoumetti K. Photovoltaic thermal (PV/T) collectors: a review. Applied Thermal Engineering 2007;27: 275–86.
[131] Kostić LjT TM, Pavlović ZT. Optimal design of orientation of PV/T collector with reflectors. Applied Energy 2010;87:3023–9.
[132] Othman MY, Yatim B, Sopian K, Bakar MNA. Performance analysis of a double-pass photovoltaic/thermal (PV/T) solar collector with CPC and fins. Renewable Energy 2005;30:2005–17.
[133] Zondag HA. Flat-plate PV-Thermal collectors and systems: a review. Renewable and Sustainable Energy Reviews 2008;12:891–959.
[134] Tiwari A, Sodha MS, Chandra A, Joshi JC. Performance evaluation of photovoltaic thermal solar air collector for composite climate of India. Solar Energy Materials and Solar Cells 2006;90:175–89.

[135] Aste N, Chiesa G, Verri F. Design, development and performance monitoring of a photovoltaic-thermal (PVT) air collector. Renewable Energy 2008;33:914–27.
[136] Sandnes B, Rekstad J. A photovoltaic/thermal (PV/T) collector with a polymer absorber plate. Experimental study and analytical model. Solar Energy 2002;72:63–73.
[137] Zondag HA, de Vries DW, WGJ van Helden, van Zolingen RJC, van Steenhoven AA. The yield of different combined PV-thermal collector designs. Solar Energy 2003;74:253–69.
[138] Gaur MK, Tiwari GN. Optimization of number of collectors for integrated PV/T hybrid active solar still. Applied Energy 2010;87:1763–72.
[139] Lazarov V, Schaeffer C, Shishkov M, Ivanova M. Hybrid solar collector. Journal of Materials Processing Technology 2005;161:229–33.
[140] Assoa YB, Menezo C, Fraisse G, Yezou R, Brau J. Study of a new concept of photovoltaic–thermal hybrid collector. Solar Energy 2007;81:1132–43.
[141] Saitoh H, Hamada Y, Kubota H, Nakamura M, Ochifuji K, Yokoyama S, et al. Field experiments and analyses on a hybrid solar collector. Applied Thermal Engineering 2003;23:2089–105.
[142] Fujisawa T, Tani T. Annual exergy evaluation on photovoltaic-thermal hybrid collector. Solar Energy Materials and Solar Cells 1997;47:135–48.
[143] Dubey S, Solanki SC, Tiwari A. Energy and exergy analysis of PV/T air collectors connected in series. Energy and Buildings 2009;41:863–70.
[144] Hegazy AA. Comparative study of the performances of four photovoltaic/thermal solar air collectors. Energy Conversion and Management 2000;41:861–81.
[145] Sarhaddi F, Farahat S, Ajam H, Behzadmehr A. Exergetic performance assessment of a solar photovoltaic thermal (PV/T) air collector. Energy and Buildings 2010;42:2184–99.
[146] Othman MY, Yatim B, Sopian K, Bakar MNA. Performance studies on a finned double-pass photovoltaic-thermal (PV/T) solar collector. Desalination 2007;209:43–9.
[147] Garg HP, Adhikari RS. System performance studies on a photovoltaic/thermal (PV/T) air heating collector. Renewable Energy 1999;16: 725–730.
[148] Solanki SC, Dubey S, Tiwari A. Indoor simulation and testing of photovoltaic thermal (PV/T) air collectors. Applied Energy 2009;86:2421–8.
[149] Sarhaddi F, Farahat S, Ajam H, Behzadmehr A, Adeli MM. An improved thermal and electrical model for a solar photovoltaic thermal (PV/T) air collector. Applied Energy 2010;87:2328–39.
[150] Alfegi MEA, Sopian K, Othman MYH, Yatim BB. Transient mathematical model of both side single pass photovoltaic thermal air collector. ARPN Journal of Engineering and Applied Sciences 2007;2:22–6.
[151] Alfegi MEA, Sopian K, Othman MYH, Yatim BB. Experimental investigation of single pass, double duct photovoltaic thermal (PV/T) air collector with CPC and fins. American Journal of Applied Sciences 2008;5:866–71.
[152] Bayrak F. Performance analysis of solar air heater with porous obstacles. Master's thesis. 2010.